Green Chemistry

ROYAL SOCIETY OF CHEMISTRY

PAPER

View Article Online
View Journal | View Issue



Cite this: *Green Chem.*, 2025, **27**, 9495

# Toughened commercial poly(L-lactide) (PLLA) using degradable and recyclable poly(ester-*alt*-ether)-*b*-PLLA†

Alexander R. Craze, Ryan. W. F. Kerr, Thomas M. McGuire, Lukas Wille and Charlotte. K. Williams *

A more sustainable future for plastics relies on the development of high performance materials that are renewably sourced, recycled without suffering losses in performance, and which are, ultimately, degradable to small molecules. Poly(L-lactide) (PLLA) is the largest scale commercial bio-derived plastic, and fulfills many of the above criteria, but is too brittle. Tackling this limitation could allow it to become a substitute for some engineering petrochemical plastics like high impact polystyrene (HIPS) or poly(acrylonitrile-butadiene-styrene) (ABS) which are not recyclable and cannot be easily defossilised. This study focusses on a series of new block polymers as rubber tougheners enabling such PLLA ductility. These block polymers are efficiently synthesised using controlled polymerizations. They are also fully chemically recyclable and biodegradable. The series of new poly(ester-*alt*-ethers)-*b*-PLLA show controllable monomer compositions, block ratios and molar mass. They are synthesised using a one-pot switchable catalysis from epoxides, anhydrides and L-lactide, using a well-controlled Zr(IV) catalyst, which selectively forms the poly(ester-*alt*-ether)-*b*-PLLA in high yield. The block polymers are blended, using systematically controlled weight percentages, with commercial, semi-crystalline PLLA ($M_n$ = 103 kg mol$^{-1}$, $Đ$ = 1.81). The PLLA blends are comprehensively evaluated using thermal analyses, melt rheology, dynamic mechanical analyses and by tensile mechanical analyses – all techniques show the promise of the new rubber tougheners in improving PLLA properties. The best performing material, featuring 15 wt% block polymer (11 wt% poly(ester-*alt*-ether)), combines the beneficial high modulus ($E$ = 3.1 ± 0.1 GPa) and high tensile strength ($\sigma$ = 48.7 ± 1.2 MPa) of PLLA with higher ductility (7× higher than PLLA, $\varepsilon_B$ = 24.5 ± 4.6%) and greater tensile toughness (8× PLLA, $U_T$ = 10.8 ± 2.2 MJ m$^{-3}$). Its mechanical properties are improved without compromise to the PLLA thermal properties, as evidenced by very similar glass transition temperature, crystallinity and melt temperature. The PLLA/block polymer blend (15 wt%) shows a lower melt viscosity (3789 Pa s$^{-1}$ *vs.* 10 335 Pa s$^{-1}$ for PLLA) and earlier onset of shear thinning, facilitating its processing. The PLLA blends are efficiently chemically recycled, using a solid state catalysed process, to L-lactide (87% yield, 100% L-LA selectivity) and the starting poly(ester-*alt*-ethers)-*b*-PLLA, facilitating its reuse in blending. The blend components, including the block polymer, are enzymatically degraded, at 37 °C, using *Humicola insolens* Cutinase over 25 days (HiC, trademark name Novozyme 51032). The properties of these toughened PLLA samples are discussed as replacements for poly(acrylonitrile butadiene styrene) (ABS) and high impact polystyrene (HIPS). In contrast to these petrochemicals, the PLLA blends are bio-derived, fully recyclable and enzymatically degradable after use.

Received 8th May 2025,
Accepted 23rd June 2025

DOI: 10.1039/d5gc02301g

rsc.li/greenchem

## Green foundation

1. Properties of bio-derived poly(L-lactide) (PLLA) are improved by adding low quantities of poly(ester-*alt*-ether)-*b*-PLLA. The blended samples undergo efficient chemical recycling and enzymatic hydrolysis. The new materials compete mechanically with acrylonitrile-butadiene-styrene and high impact polystyrene grades; in contrast to the PLLA blends these encumbant plastics are very hard to recycle.

*Department of Chemistry, University of Oxford, Chemistry Research Laboratory, 12 Mansfield Road, Oxford OX1 3TA, UK. E-mail: charlotte.williams@chem.ox.ac.uk*

† Electronic supplementary information (ESI) available. See DOI: https://doi.org/10.1039/d5gc02301g

2. Selective and efficient catalysis produces poly(ester-*alt*-ethers)-*b*-PLLA, which when blended at 15 wt% into commercial PLLA show high strength and elasticity, resulting in significantly improved tensile toughness. The blends are fully chemically recycled, at low temperatures, to L-lactide monomer and the block copolymer. All blend components are enzymatically degradable at 37 °C.
3. Future areas to address: Optimisation of the block polymer composition, structure and loading fraction in PLLA. Systems analysis, including LCA.



## Introduction

Plastics are essential in applications such as transport, construction, electronics, agriculture and house-hold products.[1,2] Despite their utility, there are major environmental concerns associated with their widespread use: firstly, their production consumes large-amounts of fossil (oil/gas) raw materials resulting in untenable greenhouse gas emissions, ~1.8 Gt (~4%) global $CO_2$ emissions. Secondly, plastic end-life treatments are limited, with very low global recycling rates, pollution from incineration and environmental pollution through formation of micro/nano-plastics.[2,4–6] Polystyrene (PS) is a top-7 petrochemical plastic, produced on ~30 Mt per annum scale.[5–7] PS is strong (tensile strength, $\sigma$ = 34–44 MPa) and stiff (Youngs modulus, $E$ = 1.9–2.4 GPa) but it is very brittle (elongation at break, $\varepsilon_B \sim 6\%$).[8] Applications requiring toughness, and ductility, are delivered by PS co- and graft polymers with butadiene, *e.g.* poly(acrylonitrile-butadiene-styrene) (ABS) and high-impact polystyrene (HIPS).[7] These toughened PS grades are widely used in construction, transport and electronics. For example, HIPS accounts for 30–40% of overall PS markets and is a major constituent (~42%) of waste electronic and electrical items.[7,9–12] As a consequence of the complex chemistries and structures of ABS and HIPS they are very difficult to recycle, either mechanically or chemically, and they are not (bio) degradable.[13,14] Overall rates of PS recycling are very low, with only ~1% of post-consumer PS waste being successfully recycled worldwide, and, unfortunately, PS contributes to ~30% of plastic landfill waste.[9,10]

One strategy to tackle these inter-linked problems is to design alternative polymers to meet the properties of toughened PS grades (ABS or HIPS) but which are derived from biomass or renewable feedstocks (to reduce greenhouse gas emissions) and which are designed for efficient and effective low-energy recycling and, ultimately, for (bio)degradation.[6,15,16] There is a growing demand and interest in such bio-based, recyclable and (bio)degradable polymers, and amongst these materials poly(L-lactide) is the largest scale commercial bio-derived plastic.[3,17,18] PLLA is already used as a sustainable alternative to PS in some applications, since it shows rather similar tensile strength and stiffness.[18,24] So far, it cannot challenge high-impact grades like HIPS or ABS.

PLLA is derived from high-starch content biomass, such as sugarcane. After use it is both mechanically and chemically recyclable.[19] For applications where it is irretrievable after use, it is also fully compostable and biodegradable.[15] Whilst there are several stereo-chemistries for polylactide, this work focuses only on the major commercial product, PLLA, which derives from L-lactide (L-LA). PLLA is the higher performing material, since its crystalline domains result in high tensile modulus ($E \sim 3.8$ GPa) and strength ($\sigma$ = 47–66 MPa).[20–22] PLLA has a moderate glass transition temperature ($T_g \sim 60$ °C), but a relatively high melting temperature ($T_m$ = 150–170 °C) and reasonable thermal stability ($T_{d5\%}$ = 215–285 °C).[23] Nonetheless, some applications are limited by its brittleness, reflected in a very low tensile toughness (<5 MJ $m^{-3}$) and low elongation at break (<5%).[21,25] These limitations arise from relatively low crack initiation and propagation energies, which often result in failure by crazing rather than shear yielding.[26] Significant research has focused on improving its ductility without loss of advantageous thermal-mechanical properties.[21,25] A major challenge is to toughen PLLA sufficiently without compromising upon its recyclability and (bio)degradability.

A range of approaches have been used to toughening PLLA, including post-polymerization backbone functionalization, use of nucleating agents, chain orientation strategies, copolymerisation, addition of small-molecule plasticisers, rubber toughening, reactive blending or crosslinking and organic/inorganic fillers.[21,25] Blending small-molecule plasticisers is perhaps the most straightforward solution in the short-term, but the resulting mixtures often phase separate over time, re-forming brittle samples.[21,27] Small molecule plasticisers also reduce the glass transition temperature, tensile strength and stiffness, which are undesirable for many applications.[21] Further, it's been shown that common plasticizers may leach from PLLA samples under environmental conditions, giving rise to concerns, as these additives may be toxic.[28]

An alternative is the blending of small quantities of elastomeric polymers into PLLA, known as rubber toughening.[21,29] When using miscible polymer elastomer/PLLA blends, the elongation at break can increase significantly, but with the trade-off of compromised strength and decreased glass transition temperature.[26] When using immiscible elastomeric polymers, the blends show micron sized elastomer aggregates or particles dispersed in the PLLA. These particles are believed to function as stress concentrators, promoting plastic deformation and toughening. Optimising the particle sizes and separations helps overlap their stress fields, promoting energy dissipation.[25,30] Such immiscible blends often also require another additive, a compatibilizer, to stabilise the PLLA-elastomer interface and prevent particle coalescence over time.[31]

Amphiphilic block polymers, combining elastomeric and PLLA-miscible blocks, are very useful toughening agents, providing both dispersed elastomeric phases and stable interfaces. They also show better control over dispersed particle sizes; in some cases, their use results in ultra-tough PLLA.[20,31–37] One issue is that most of these amphiphilic block polymers feature pervasive polymer chemistries. Given that one of the major benefits of PLLA is its better end-life options, amphiphilic block polymers which are both recyclable and degradable are important.

 

This work describes a new approach to block polymer rubber toughening using poly(ester-*alt*-ether)-*b*-PLLA structures. Importantly, both blocks feature repeat units containing aliphatic ester linkages which should help ensure the overall material is (bio)degradable (Scheme 1). The block polymer synthesis is designed to exploit controlled and selective polymerization catalysis, starting from common commercial monomers: epoxides, anhydrides and L-lactide. We selected the elastomeric poly(ester-*alt*-ether) block following a recent discovery, from our team, of a Zr(IV) catalyst showing very unusual selectivity in copolymerization of epoxides and anhydrides, producing polymers featuring anhydride-epoxide-epoxide, or ester-*alt*-ether, sequences.[38] In 2024, we showed that this controlled polymerization catalysis was applicable to a range of epoxides and anhydrides and could even deliver poly(ester-*alt*-ethers) with the desirable low $T_g$ values needed in an elastomer block ($-60 < T_g < 25$ °C).[39] Proof of concept chemical degradation (pH = 14, aqueous conditions) revealed that the poly(ester-*alt*-ethers) degraded faster than equivalent alternating polyesters motivating their testing in enzymatic degradation (biodegradation) conditions in this work.[38] To make the target amphiphilic block polymers, the polymerization catalysis must be developed to selectively copolymerize poly(ester-*alt*-ethers) and PLLA blocks, the latter selected to deliver PLLA matrix compatibility.

## Results

### Poly(ester-*alt*-ether)-*b*-PLLA synthesis

A series of block polymers, poly(ester-*alt*-ether)-*b*-PLLA, were synthesised using a using a Zr(IV) catalyst, **1**, applied in a one-pot, sequential monomer addition process. In the first step, the catalysed ring opening copolymerization (ROCOP) of either diglycolic anhydride or maleic anhydride (DGA or MA) with *racemic* 1,2-epoxy-9-decene (ED) produced the poly(ester-*alt*-ether) block, and, in the second step, the same catalyst was used for the controlled ring-opening polymerization (ROP) of L-lactide.[38] There are benefits to using commercial monomers and single reactor processes, not least as these syntheses circumvent isolation of intermediates or use of macro-initiators.[40] To exemplify the typical conditions used to make the poly(ester-*alt*-ethers), the synthesis of **P1** from MA and ED is described here (full details for the other polymers are provided in the ESI, Fig. 1†).[39] All polymerisations were performed using [**1**]:[Anhydride]:[Epoxide] = 1:50:546, at 50 °C. As demonstrated in our previous work, both of the iso-propoxide ligands of catalyst **1** initiate the polymerization, forming a poly(ester-*alt*-ether) with a degree of polymerisation (DP) of 25, after complete anhydride conversion. This was demonstrated (previously), using phthalic anhydride (PA) and butylene oxide (BO), by $^1$H NMR spectroscopy (the iso-propoxide end-group showed a distinctive signal from the shorter epoxide side-chains in this instance) as well as by stoichiometric addition of PA and catalyst (in toluene at 80 °C for 24 h) and analysis by mass spectrometry and $^1$H NMR spectroscopy.[38,39] Later, for the monomer combination MA/BO, with purposely low molar mass samples, the iso-propoxide end-group was observed by MALDI-TOF.[39]

The poly(ester-*alt*-ether) sequence was characterised using a combination of NMR spectroscopy, GPC and thermal methods.[38,39] For example, the $^1$H NMR spectrum for **P1** clearly shows resonances assigned to protons adjacent to both

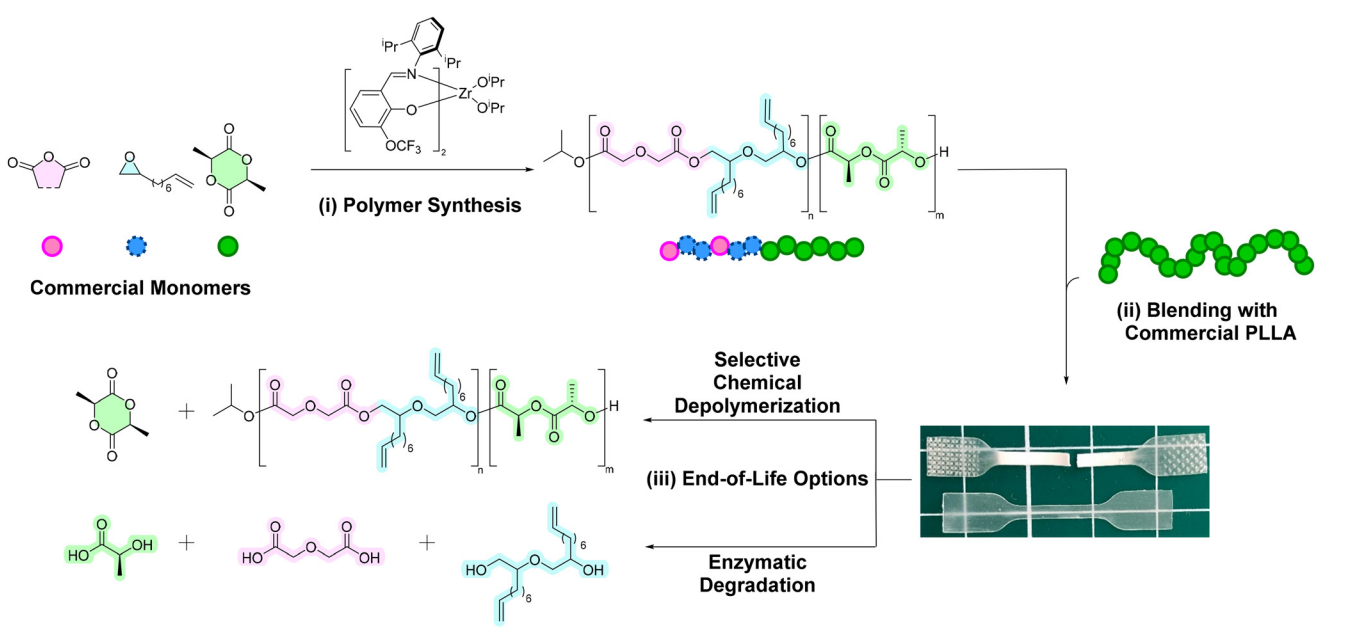


**Scheme 1** The strategy for producing poly(ester-*alt*-ethers) used to toughen commercial, semi-crystalline PLLA. The approach in this work includes: (i) synthesis of poly(ester-*alt*-ether)-*b*-PLLA block copolymers, (ii) blending with commercial PLLA and (iii) developing chemical recycling and enzymatic degradation processes.

ester ($\delta_H$ = 4.99 and 4.16 ppm, respectively) and ether ($\delta_H$ = 3.88–3.18 ppm) groups (Fig. S3†). In the COSY NMR spectrum, the ester resonances do not show any correlations to one another, but do correlate with resonances in the ether region (Fig. S5 and S6†). To compare, the alternating polyester prepared from the same monomers **P1′** (DP = 25, synthesised using catalyst **2**, Fig. S2†) did not show any ether signals in its $^1$H NMR spectrum (Fig. S8–10†). Also, **P1′** shows the methine-ester resonance at higher chemical shift (5.13 ppm) than the equivalent signal for **P1** (4.99 ppm, Fig. S10 and S6† respectively). For **P1′**, the $^1$H COSY NMR spectrum shows clear correlations between the methine-ester and methylene-ester resonances, which is quite different to **P1** (Fig. S10,† resonances 1′–2′). The poly(ester-*alt*-ether) **P1** shows a molar mass, determined by GPC, which is consistent with theoretical predictions and a narrow dispersity, monomodal distribution (Table 1). **P1** is amorphous with a glass transition temperature of −50 °C (*vs.* **P1′**, $T_g$ = −41 °C) consistent with the enhanced segmental motion afforded by the ether linkages (Table 1 and Fig. S64†). Following the same experimental conditions, a series of new poly(ester-*alt*-ethers) were prepared and all showed NMR spectroscopic characterization data consistent with the repeat unit sequences and experimental $M_n$ values close to theoretical values (10.3 < $M_n$ < 11.5 kg mol$^{-1}$) with narrow dispersities (1.12 < $Đ$ < 1.24) (Table 1). The poly(ester-*alt*-ether)-*b*-PLLA copolymers were all synthesised by a sequential addition process, whereby L-LA was added into the reaction after complete conversion of the anhydride monomers in the ROCOP (Fig. 1a). For example, **P1-PLLA** prepared using the polymerization conditions outlined above ([**1**] = 0.01 M, neat ED, 50 °C) showed rapid MA/ED copolymerization (complete MA conversion in <55 min, $k_{obs}$ = 54 M min$^{-1}$), forming the **P1** block, with a DP(MA) of 25 and DP(ED) of 59 (Fig. 1b). The MA : ED ratio stayed at 1 : 2, throughout the reaction, as expected for selective poly(ester-*alt*-ether) formation (Fig. 1d). After complete anhydride (MA) consumption, the addition of L-LA initiated a mechanistic switch into L-LA ROP (Fig. 1b and Fig. S22† illustrates switch catalysis). The ROP of L-LA occurred more slowly ($k_{obs}$ = 2.0 × 10$^{-3}$ min$^{-1}$) reaching complete conversion, DP(PLLA) = 27, after 30 hours (Fig. 1b). Conducting the polymerizations with regular aliquot analyses enabled plots of conversion *vs.* time data. There is a linear increase in poly(ester-*alt*-ether) concentration (1-[MA]) over time. This data is consistent with rates being zero order in anhydride concentration, as was found in prior kinetic analyses of epoxide/anhydride copolymerisations using catalyst **1**.[38] In contrast, the PLLA concentration (1-[L-LA]) increases exponentially over time, consistent with rates being first order in [L-LA] (Fig. 1b).

**Table 1** Overview of poly(ester-*alt*-ether)-*b*-PLLA synthesis and characterisation data[a]

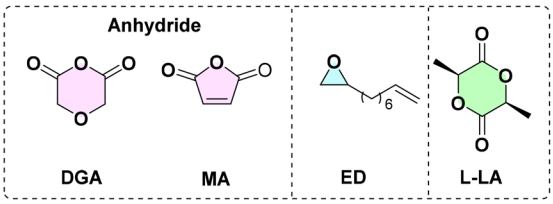


| Entry | Polymer | Monomer stoichiometry [Cat] : [Anhy] : [ED] : [L-LA] | Block polymer DP [Anhy] : [ED] : [L-LA][b] | Block polymer $w_{PLLA}$[c] (%) | $M_n$($Đ$)[d] [kg mol$^{-1}$] | $M_n$[e] (theo.) | $T_g$[f] (°C) |
|---|---|---|---|---|---|---|---|
| 1 | **P1 P(MA-ED-ED)** | 1 : 50 : 546 : 0 | 25 : 50 : 0 | 0 | 11.5(1.12) | 10.2 | −50 |
| 2 | **P1**[g] **P(MA-ED)** | 1 : 25 : 546 : 0 | 24 : 30 : 0 | 0 | 3.5(1.52) | 7.5 | −41 |
| 3 | **P1$_{25}$-PLLA$_{27}$** | 1 : 50 : 546 : 50 | 25 : 59 : 27 | 0.25 | 17.0(1.22) | 15.8 | −47 |
| 4 | **P1$_{25}$-PLLA$_{18}$***[h] | 1 : 50 : 546 : 50 | 25 : 60 : 18 | 0.18 | 14.2(1.13) | 14.4 | −44 |
| 5 | **P2 P(DGA-ED-ED)** | 1 : 50 : 546 : 0 | 25 : 54 : 0 | 0 | 10.3(1.24) | 11.3 | −51 |
| 6 | **P2$_{25}$-PLLA$_{23}$** | 1 : 50 : 546 : 50 | 25 : 56 : 23 | 0.26 | 16.9(1.28) | 14.9 | −46 |
| 7 | **P2$_{25}$-PLLA$_{68}$** | 1 : 50 : 546 : 150 | 25 : 49 : 68 | 0.49 | 23.6(1.63) | 20.3 | −45 |
| 8 | **P2$_{25}$-PLLA$_{125}$** | 1 : 50 : 546 : 250 | 25 : 53 : 125 | 0.62 | 24.1(1.48) | 29.2 | −43, 48 |
| 9 | **P2$_8$-PLLA$_{26}$** | 1 : 15 : 546 : 50 | 8 : 18 : 26 | 0.55 | 8.9(1.27) | 7.7 | −40 |
| 10 | **P2$_{15}$-PLLA$_{27}$** | 1 : 30 : 546 : 50 | 15 : 36 : 27 | 0.35 | 6.9(1.17) | 11.2 | −40 |
| 11 | **P2$_8$-PLLA$_9$** | 1 : 15 : 546 : 15 | 8 : 16 : 9 | 0.30 | 5.7(1.17) | 4.8 | −45 |
| 12 | **P2$_{12}$-PLLA$_{15}$** | 1 : 25 : 546 : 25 | 12 : 24 : 15 | 0.32 | 8.5(1.34) | 7.3 | −46 |

[a] Reaction conditions: [**1**] = 10 mM in 1 mL epoxide (note ED is racemic), 50 °C (Fig. 1a and Fig. S2† for catalyst structure). [b] DP of anhydride was measured by monomer conversion data by integration of the monomer and polymer resonances in the $^1$H NMR spectra of crude polymers (Fig. S3†). It is assumed both isopropoxide ligands initiate polymerisation. DP of ED and L-LA were determined by integration of the $^1$H NMR spectra of purified polymer against the anhydride polymer resonance. [c] Weight fraction of PLLA blocks ($w_{PLLA}$) calculated based on monomer DP values from $^1$H NMR spectra. [d] Determined by gel permeation chromatography (GPC), using THF as the eluent, and calibrated using narrow MW polystyrene standards. [e] Theoretical $M_n$ values were calculated from the monomer conversion data and assume both isopropoxides initiate. [f] Obtained from differential scanning calorimetry (DSC, third heating cycle, 10 °C min$^{-1}$ heating rate). [g] Reaction conditions: [**2**] = 10 mM in neat 1 mL epoxide (see Fig. S2† for catalyst structure). [h] One pot synthesis of monomer mixture (switch polymerization catalysis).

 

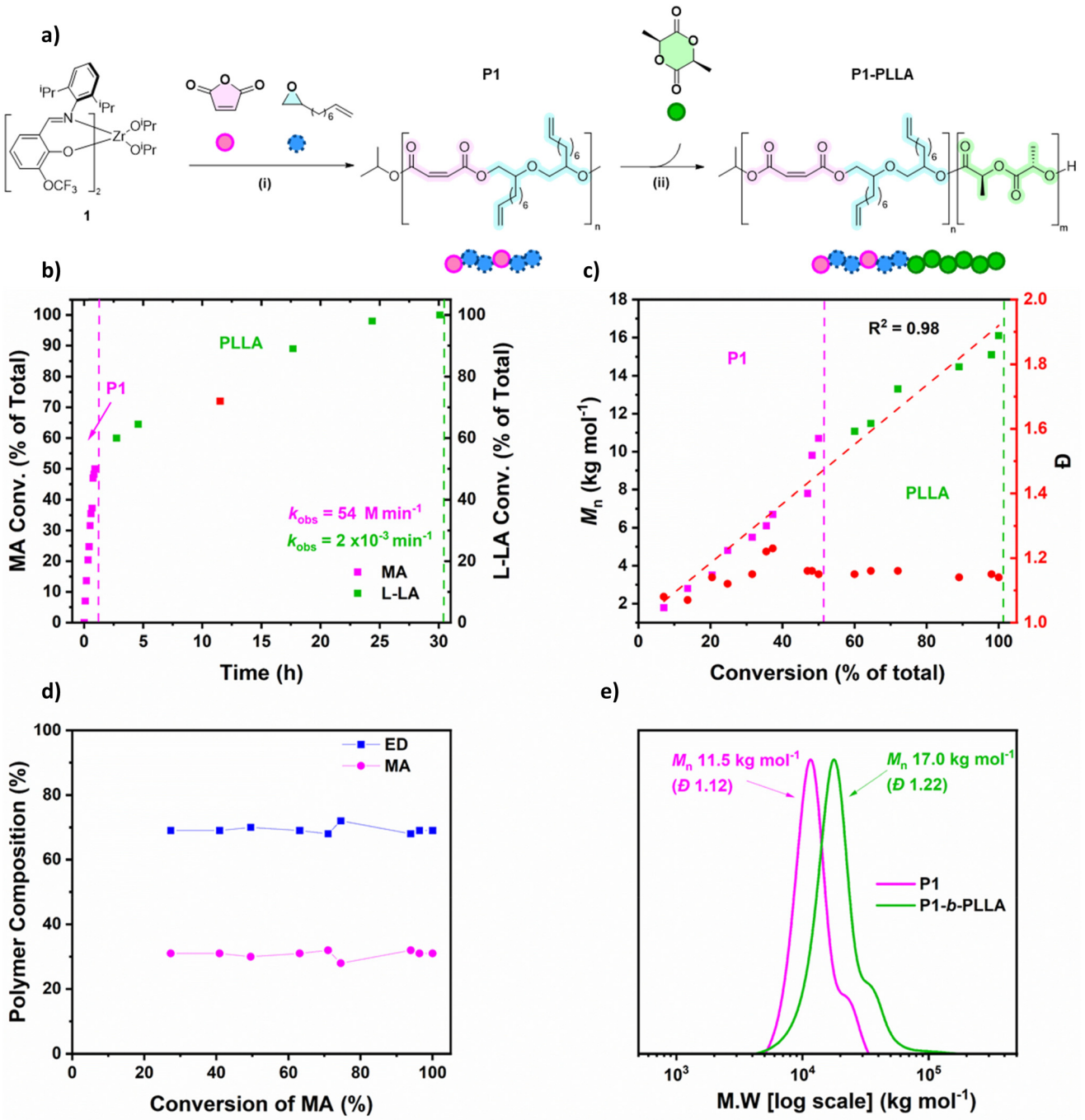


**Fig. 1** Synthesis of poly(ester-*alt*-ether)-*b*-PLLA block polymers using catalyst **1**. (a) (i) The copolymerization of MA/ED, conditions: $[MA]_0$ = 0.5 mM (50 equivalents), 50 °C in 1 mL epoxide (546 equivalents for ED), [**1**] = 0.01 mM (one equivalent); (ii) L-LA polymerization, conditions: as before. The overall monomer stoichiometry is [**1**] : [MA] : [ED] : [L-LA] = 1 : 50 : 546 : 50. (b) Conversion *vs.* time data for **P1-PLLA** formation, demonstrating MA (pink squares) and L-LA (green squares) conversion (normalised by overall maximum monomer conversion). The pseudo rate coefficients, $k_{obs}$, were determined as the gradient of the [MA] *vs.* time (min) for MA/ED ROCOP and the gradient of a plot of ln([L-LA]/[L-LA]$_0$) *vs.* time (min) for L-LA ROP. (c) Plot showing **P1-PLLA** $M_n$ and *Đ* *vs.* monomer conversion. Data for the MA/ED ROCOP (pink), and then L-LA ROP (green). (d) Plot showing **P1** composition *vs.* polymer conversion, with MA (pink) and ED (blue) conversions determined by $^1$H NMR spectroscopy (Table 1). (e) GPC data for aliquots collected during **P1-PLLA** synthesis. The data show **P1** formation (>99% conversion, pink) and, later, **P1-PLLA** formation (>99% L-LA conversion, green).

The block polymers were analysed using a range of techniques, including by $^1$H NMR spectroscopy, GPC and DSC methods. For **P1-PLLA**, the $^1$H and $^{13}$C{$^1$H} NMR spectra show resonances for both blocks. In particular, the $^{13}$C{$^1$H} NMR spectrum displays carbonyl resonances assigned to **P1** poly(ester-*alt*-ether) at 165 ppm and PLLA at 169 ppm. There are no other car-

bonyl signals, which is a good indicator of selective block polymer formation and suggests that any transesterification side-reactions occur more slowly than block propagation (Fig. S15†).[41] Further evidence for block polymer formation comes from molecular weight (GPC) analyses of reaction aliquots, which show steadily increasing polymer $M_n$ with polymer conversion and narrow dispersity values ($Đ$ < 1.25, Fig. 1c). The block polymers showed $M_n$ values, by GPC, which were in close agreement with theoretical values (Table 1). In a few of the GPC traces, there were low intensity higher shoulder peaks which are attributed to block polymers, that, rather than being catalyst initiated, are produced from low quantities of diol/diacid present in the monomers (Fig. 1e and Fig. S61–63†). The DOSY NMR spectra show a single diffusion coefficient, consistent with block polymer formation (section S4.1†).

One-pot polymerizations using monomer mixtures are attractive, in terms of green chemistry, as they prevent additional reaction steps, obviate additional catalysts, solvents and purifications of pre-polymers/macro-initiators. Such processes also simplify larger-scale polymerization processes. One such route, is a form of switchable catalysis, which selectively enchains mixtures of epoxides, anhydrides and cyclic esters to form block polyesters.[42,43] The rules for these switchable catalyses are quite generally applicable and predict that from the monomer mixtures, the epoxide/anhydride ROCOP occurs first (forming a polyester) and is followed selectively by lactone ROP (also forming a polyester) only after complete anhydride consumption.[40] It is not clear whether catalyst **1**, which forms poly(ester-*alt*-ethers) from epoxides/anhydrides, should follow the same selectivity rules. To investigate its potential in switchable polymerization catalysis, a mixture of MA/ED/L-LA was reacted with catalyst **1**, under identical conditions to those used above. The polymerization was monitored by regular removal of aliquots which were analysed by $^1$H NMR spectroscopy (Fig. 2a and b). Over 2 h, only the anhydride and epoxide were consumed, selectively forming the poly(ester-*alt*-ether). The concentration of [MA] showed a linear decrease with time, once again consistent with rates that are zero order in anhydride concentration ($k_{obs}$ = 1.45 M min$^{-1}$). After 2 h, and once anhydride consumption was >95%, the ROP of L-LA started and PLLA resonances were observed in the reaction aliquots. PLLA synthesis was significantly slower than the poly(ester-*alt*-ether) block and showed a first order rate dependence on L-LA concentration ($k_{obs}$ = 4.6 × 10$^{-4}$ min$^{-1}$). The aliquots were also analysed by GPC and showed steady increases to polymer $M_n$ with monomer conversion; throughout the reaction, samples showed monomodal molecular weight distributions and narrow dispersity values ($Đ$ < 1.2). The switchable catalysis resulted in the formation of a very similar/identical block polymer, **P1-PLLA***, to the material produced by the sequential addition process. For example, its DOSY NMR spectrum also showed a single diffusion coefficient, indicative of a block polymer (Fig. S21†). The thermal properties of the two block polymers, **P1-PLLA** and **P1-PLLA***, are very similar (*e.g.* $T_g$ = −47 and −44 °C, respectively; $T_{d,5}/T_{d,95}$ = 237/499 and 255/500 °C, respectively) (Table 1 and Fig. S64, S67†). End-group analysis, using $^{31}$P{$^1$H} NMR spectroscopy titration methods, showed only PLLA resonances consistent with the block polymer structure (Fig. S24 and S25†). The experiment suggests that mixtures of monomers can be enchained by switchable catalysis to prepare the desired block polymers. The selectivity, from the monomer mixtures, is tentatively attributed to the alkoxide intermediate, formed during catalysis using Zr(IV)

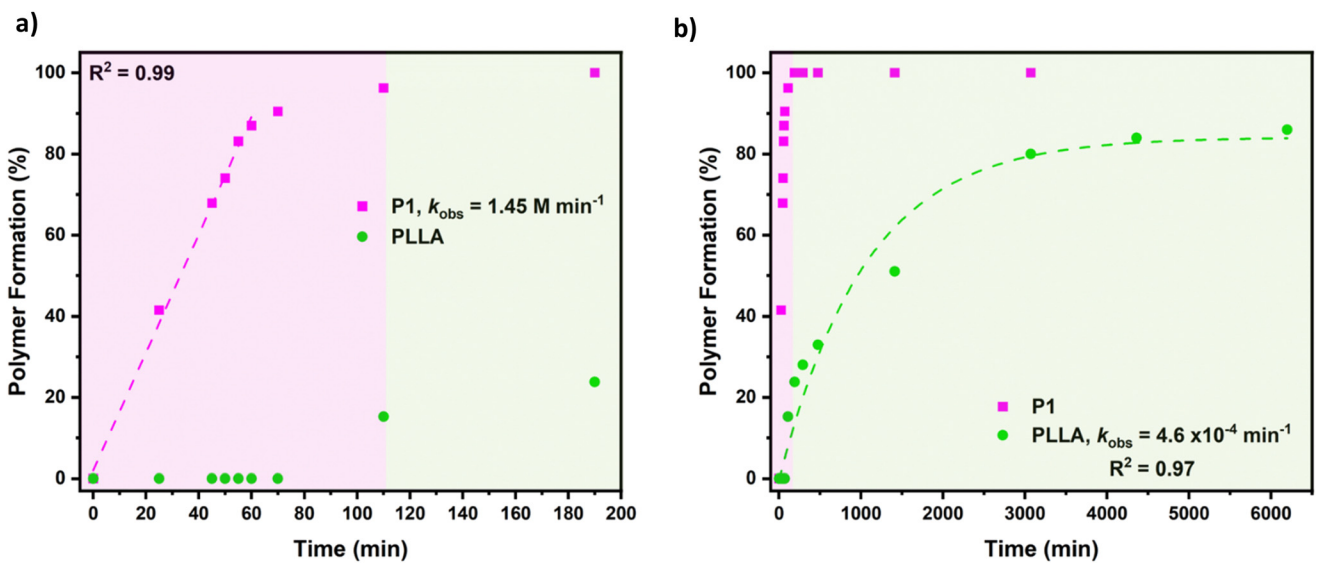


Fig. 2 Shows conversion *vs.* time data for the switchable polymerization catalysis using mixtures of MA, ED and L-LA to form **P1-PLLA*** (a) Plot showing **P1** formation (% conversion) *vs.* time, with linear fit to experimental data. Plot also shows that after 110 min, **PLLA** block formation starts. (b) Plot showing block polymer formation (% conversion) *vs.* time focusing on the PLLA block formation (110–6000 min). The experimental data are fit by exponential growth kinetics. Reaction conditions: [**1**] = 10 mM (1 equiv.), in neat 1 mL epoxide (546 equiv.), 50 equiv. MA and L-LA, respectively. The pseudo rate coefficients, $k_{obs}$, were determined as the gradient of the [MA] *vs.* time (min) for MA/ED ROCOP and the gradient of a plot of ln([L-LA]/[L-LA]$_0$) *vs.* time (min) for L-LA ROP.

 

catalyst **1**, showing faster and more stable anhydride insertions compared with the competitive L-lactide insertions.[38,40] Although the use of mixtures and switchable catalyses could be useful in future for larger-scale processes, for consistency in this work, all the other block polymers were produced by sequential L-LA addition methods. Accordingly, a series of block polymers were prepared, with focus on polymerizations of DGA/ED (**P2**)/L-LA. By systematically controlling the relative monomer concentrations and conversions, a series of **P2$_x$-PLLA$_y$** samples were prepared featuring different block ratios/compositions (DP and weight fraction PLLA) and molecular weights ($M_n$, Table 1).

### PLLA + block polymer blends

The poly(ester-*alt*-ether)-*b*-PLLA copolymers were blended into PLLA and the materials' thermal and mechanical properties were compared to the pure PLLA sample (Table 2 and Fig. 3). For these experiments, a commercial, high molecular weight semi-crystalline PLLA sample was selected, since it should deliver the greatest mechanical strength, but such samples are more challenging to toughen than amorphous PLA (PLLA, Goodfellow, ME34-GL-000110, $M_n$ = 103 kg mol$^{-1}$, $Đ$ = 1.81, from GPC in $CHCl_3$). The blends were prepared, on a lab-scale, by solvent casting the **P2$_x$-PLLA$_y$** samples with commercial PLLA (using minimum amountsof $CH_2Cl_2$). After drying (under vacuum, 60 °C, 2 days), the blends were heated to 180 °C, for 10 minutes (above PLLA melting temperature), and slowly cooled (overnight, see section S3.0† for polymer blend procedure). This process formed highly transparent, colourless films. The films were visibly homogeneous, free of air bubbles (Fig. S1†) and processing solvent (Fig. S74–77†). The films all showed similar, reproducible thicknesses from 0.15–0.30 mm. It's important to emphasise these PLLA processing conditions are best suited to lab-scale testing, and to ensure fair comparisons between materials, but would not be used at scale where solvent-free compounding and extrusion processing would be preferable. Firstly, the blend composition influences over properties were assessed, using systematically increasing quantities of **P2$_{25}$-PLLA$_{23}$**: 1, 2, 5, 7.5, 10, 15, 20 and 25 wt% *vs.* the PLLA matrix (Table 2). Henceforth, these blends will be represented by labels **[P2$_x$-PLLA$_y$]$_z$**, where $x$ = DP **P2**, $y$ = DP PLLA, $z$ = wt% added to the PLLA blend (Table 2, entries 4–17).

### Thermal properties

The first series of blends comprise systematically increasing amounts of the 50 : 50 composition **P2$_{25}$-PLLA$_{23}$** block polymer in PLLA (Table 2, entries 4–11). The blend thermal properties are all very similar to neat PLLA, which is encouraging since it suggests the elastomeric poly(ester-*alt*-ether) blocks are immiscible in PLLA and may suggest block polymer phase separation in the blend. For the series, the blend materials' glass transition

**Table 2** Summary of thermal and mechanical properties of a series of poly(ester-*alt*-ether)-*b*-PLLA and PLLA blends[a]

| Entry | Blend | $\chi$[b] (%) | $T_g$[b] (°C) | $T_m$[b] (°C) | $T_{d,5}$[c] (°C) | $E$[d] (GPa) | $\sigma_Y$[d] (MPa) | $\varepsilon_B$[d] (%) | $U_T$[d] (MJ m$^{-3}$) |
|---|---|---|---|---|---|---|---|---|---|
| 1 | **PLLA** | 34 | 65 | 149 | 321 | 2.9 ± 0.3 | 66.7 ± 4.3 | 3.4 ± 0.5 | 1.4 ± 0.3 |
| 2 | **[P1$_{25}$-PLLA$_{27}$]$_{7.5}$** | 46 | 64 | 148 | 279 | 3.4 ± 0.1 | 59.2 ± 2.6 | 6.6 ± 1.5 | 3.2 ± 0.8 |
| 3 | **[P2]$_{7.5}$** | 35 | 65 | 150 | 294 | 3.2 ± 0.4 | 52.2 ± 6.2 | 4.5 ± 1.3 | 2.0 ± 0.6 |
| 4 | **[P2$_{25}$-PLLA$_{23}$]$_1$** | 41 | 64 | 149 | 317 | 3.1 ± 0.3 | 64.5 ± 5.6 | 4.2 ± 1.0 | 2.0 ± 0.6 |
| 5 | **[P2$_{25}$-PLLA$_{23}$]$_2$** | 39 | 64 | 149 | 308 | 3.3 ± 0.3 | 65.0 ± 7.1 | 3.9 ± 0.9 | 1.8 ± 0.6 |
| 6 | **[P2$_{25}$-PLLA$_{23}$]$_5$** | 39 | 64 | 152 | 296 | 3.3 ± 0.2 | 63.3 ± 4.3 | 3.7 ± 1.1 | 1.7 ± 0.7 |
| 7 | **[P2$_{25}$-PLLA$_{23}$]$_{7.5}$** | 35 | 64 | 149 | 290 | 2.9 ± 0.5 | 59.2 ± 4.8 | 9.5 ± 1.9 | 4.6 ± 1.1 |
| 8 | **[P2$_{25}$-PLLA$_{23}$]$_{10}$** | 40 | −46, 64 | 149 | 288 | 3.3 ± 0.2 | 56.4 ± 5.5 | 9.8 ± 3.0 | 4.8 ± 1.8 |
| 9 | **[P2$_{25}$-PLLA$_{23}$]$_{15}$** | 42 | −45, 63 | 149 | 291 | 3.1 ± 0.1 | 48.7 ± 1.2 | 24.5 ± 4.6 | 10.8 ± 2.2 |
| 10 | **[P2$_{25}$-PLLA$_{23}$]$_{20}$** | 37 | −47, 64 | 151 | 290 | 2.4 ± 0.2 | 35.0 ± 2.1 | 35.7 ± 3.6 | 10.8 ± 1.5 |
| 11 | **[P2$_{25}$-PLLA$_{23}$]$_{25}$** | 22 | −45, 65 | 150 | 292 | 2.3 ± 0.1 | 32.0 ± 2.0 | 20.8 ± 3.9 | 5.8 ± 0.9 |
| 12 | **[P2$_{25}$-PLLA$_{68}$]$_{15}$** | 42 | −47, 63 | 153 | 289 | 3.1 ± 0.3 | 49.4 ± 4.2 | 16.5 ± 7.2 | 6.8 ± 3.1 |
| 13 | **[P2$_{25}$-PLLA$_{125}$]$_{15}$** | 42 | −48, 64 | 154 | 288 | 3.2 ± 0.2 | 53.3 ± 2.7 | 10.7 ± 3.6 | 4.7 ± 1.8 |
| 14 | **[P2$_8$-PLLA$_{26}$]$_{15}$** | 43 | −46, 60 | 151 | 278 | 3.0 ± 0.2 | 53.1 ± 3.5 | 4.7 ± 2.5 | 1.9 ± 1.2 |
| 15 | **[P2$_{15}$-PLLA$_{27}$]$_{15}$** | 43 | −47, 60 | 150 | 295 | 2.2 ± 0.2 | 38.1 ± 2.3 | 18.5 ± 3.3 | 5.9 ± 0.9 |
| 16 | **[P2$_8$-PLLA$_9$]$_{15}$** | 44 | −46, 60 | 154 | 301 | 2.4 ± 0.2 | 37.2 ± 2.5 | 4.3 ± 1.8 | 1.2 ± 0.5 |
| 17 | **[P2$_{12}$-PLLA$_{15}$]$_{15}$** | 42 | −44, 59 | 158 | 296 | 2.7 ± 0.2 | 42.4 ± 5.2 | 18.8 ± 7.0 | 6.7 ± 2.4 |

[a] Commercial PLLA was used in blending, provided by Goodfellow ME34-GL-000110 ($M_n$ = 103.4(1.81) kg mol$^{-1}$ *vs.* polystyrene standards in $CHCl_3$). [b] Obtained from differential scanning calorimetry (DSC, first heating cycle, 10 °C min$^{-1}$ heating rate from −80 to 180 °C). The enthalpies of crystallization and melting were determined by the integrated area of the exothermic peak and endothermic peaks respectively, while the crystallization and melting temperatures were obtained from the maximum and minimum of the exo- and endothermic peaks, respectively. Crystallinity was calculated by $(\Delta H_m - \Delta H_{cc})/\Delta H_{m,100} \times 100$, where $\Delta H_{m,100}$ is the enthalpy of melting for 100% crystalline PLLA and is equal to 93.7 J g$^{-1}$. Below 10 wt% block polymer, the lower $T_g$ was not observable by DSC. [c] Obtained from TGA (polymer samples were heated from 30 to 700 °C at a rate of 10 °C min$^{-1}$, under $N_2$ flow 12 mL min$^{-1}$). [d] Uniaxial tensile measurements were conducted at 10 mm min$^{-1}$ extension rate. The mean values and standard deviations are calculated from measurements conducted independently on five separate specimens conforming to dimensions for ISO 527-2 type 5B. Tensile toughness was calculated from the area under the stress–strain plots. Entries 4–11 change the wt% diblock copolymer. Entries 12 and 13 are blends changing PLLA block DP, while fixing **P2** DP (Fig. S86a and b†). Entries 14 and 15 are blends changing **P2** block DP, while fixing PLLA block DP (Fig. S86a and b†). Entries 16 and 17 are blends changing the overall $M_n$, fixing DP **P2** : DP PLLA (Fig. S86c and d†). The polymer name is contained within square brackets, while the wt% of polymer additive used in the PLLA blend is the subscript on the outside of the square brackets.

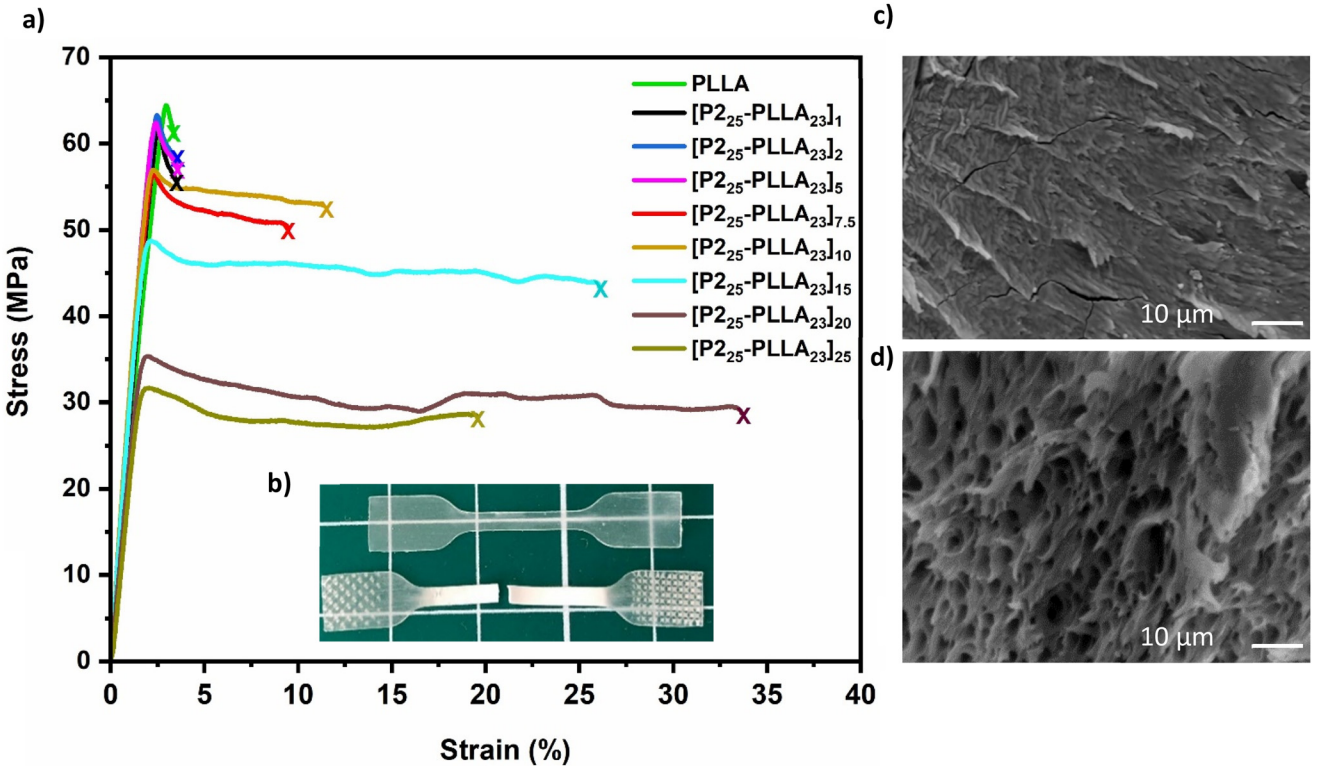


**Fig. 3** Tensile mechanical characterization of [P2$_{25}$-PLLA$_{23}$]$_z$ series, where $z$ = 1–25 wt%. (a) Plot showing sample tensile stress *versus* strain data for the series of PLLA blends and compared against neat PLLA (see Table 2 for numerical values and error analysis). (b) Photograph of the tensile specimens (ISO 527-2 type 5B) for [P2$_{25}$-PLLA$_{23}$]$_{15}$ before (top) and after (bottom) tensile failure. (c) and (d) SEM images of the fracture surfaces for neat PLLA (c) and [P2$_{25}$-PLLA$_{23}$]$_{15}$ (d) after tensile failure (sample magnification illustrated).

temperature and melting temperature values are very close to those of neat PLLA (Table 2, entry 1 *vs.* 4–11). Lower $T_g$ values could be observed between 10–25 wt% blends, although below this, the concentration is too low to observe a signal in DSC (Fig. S73†). The PLLA crystallinity ($\chi$), determined by analysis of the DSC melting transitions, shows equivalent or higher values than neat PLLA for most of the blends—important since sample crystallinity is key to providing the beneficial tensile mechanical strength and stiffness. Across the series, PLLA crystallinity values in the range 35–42% were observed, these are equivalent or slightly higher than for neat PLLA (only the highest additive loading results in decreased crystallinity). The maximum crystallinity (42%) was observed for the 15 wt% blend, [P2$_{25}$-PLLA$_{23}$]$_{15}$ (Table 2, entry 9). The samples all showed similar thermal stability to pure PLLA, with $T_{d5\%}$ values, determined by TGA, in the range 288–317 °C (Table 2, entries 1 *vs.* 4–11).

### Tensile mechanical properties

Uniaxial tensile extension experiments were performed according to ISO 527 using dumbbell-shaped specimens (ISO 527-2 type 5B, with five technical replicates, see section S1.2.3†). For 1–5 wt% blends of P2$_{25}$-PLLA$_{23}$, the tensile mechanical properties were nearly identical to PLLA and no toughening was observed (Table 2, entries 4–6; Fig. 3). At blends with >5 wt% block polymer, the elongation at break increased significantly, reaching a maximum at 36% for [P2$_{25}$-PLLA$_{23}$]$_{20}$ (Table 2, entry 10). Importantly for samples 5–15 wt%, the elongation at break was increased, but without significant compromise to the high tensile strength and stiffness.

The best performing sample was [P2$_{25}$-PLLA$_{23}$]$_{15}$, which showed a high strength ($\sigma_Y$ = 48.7 ± 1.2 MPa) and stiffness ($E$ = 3.1 ± 0.1 GPa) together with significantly increased ductility ($\varepsilon_B$ = 24.5 ± 4.6%) *vs.* neat PLLA (Table 2, entry 1 *vs.* 9). This sample showed the greatest tensile toughness (10.8 ± 2.2 MJ m$^{-3}$, Table 2 and Fig. 3a). To test the importance of the block polymer structure, a PLLA blend containing 7.5 wt% of P2 was prepared in an identical way ([P2]$_{7.5}$) (Table 2, entry 3). The sample behaved very similarly to PLLA and did not show any significant increases to elongation at break ($\varepsilon_B$ = 4.5% ± 1.3), and, low overall tensile toughness ($U_T$ = 2.0 ± 0.6 MJ m$^{-3}$). In comparison, the 7.5 wt% block polymer sample showed higher values for tensile strength (59.2 ± 4.8 MPa), double the elongation at break (9.5 ± 1.9%) and 2× greater tensile toughness (4.6 ± 1.1 MJ m$^{-3}$) than this sample (Table 2, entry 7). These findings indicate that the block polymer structure plays a significant role in delivering the PLLA toughening. A blend of 7.5 wt% P1$_{25}$-PLLA$_{27}$ ([P1$_{25}$-PLLA$_{27}$]$_{7.5}$) was also examined (Table 2, entry 2), although this copolymer was not explored any further, due to the superior performance of P2$_{25}$-PLLA$_{23}$ as the preferred additive (Table 2, entry 7).

To probe the blend composition and test whether self-assembled block polymer structures were observed, the samples were analysed using scanning electron microscopy. The SEM measurements were conducted using the fractured surfaces of four tensile specimens (with samples analysed perpendicular to the direction of uniaxial tension stress); neat PLLA, $[\mathbf{P2}_{25}\text{-}\mathbf{PLLA}_{23}]_{7.5}$, $[\mathbf{P2}_{25}\text{-}\mathbf{PLLA}_{23}]_{15}$ and $[\mathbf{P2}_{25}\text{-}\mathbf{PLLA}_{23}]_{25}$ (Fig. 3c, d and Fig. S85†). The neat PLLA sample shows an almost featureless surface, with large microcracks forming. There was no evidence for sample plastic deformation (Fig. 3c). On the other hand, the blends all showed the formation of evenly distributed micron-sized voids throughout the PLLA matrix, after fracture (Fig. 3d and Fig. S85†). As the block polymer wt% increases, so do the size of these voids, although they remain well dispersed throughout the fracture surface (Fig. S85†). There was no evidence for any remaining polymer particles in the voids. These data are indicative of mechanical failure by debonding and cavitation of the dispersed block polymer particles within the PLLA matrix. The data also suggest the toughened PLLA samples show shear yielding prior to failure (Fig. 3d and S85†).[25,32] It is proposed that once these samples reach a critical tensile strain, the block polymer particles cavitate from the matrix, which creates voids around them, reducing shear yielding energy and promoting matrix (PLLA) plastic deformation (*i.e.* rearrangement of crystalline domains in the matrix). In this way, the block polymers help prevent strain localisation and mitigate crack propagation and mechanical failure.[25,32] The blend samples fail by PLLA plastic deformation, which is observed by increases to both sample elongation at break and tensile toughness (Fig. 3a).[25,32] Examining photographs of the optimum sample, $[\mathbf{P2}_{25}\text{-}\mathbf{PLLA}_{23}]_{15}$, before and after tensile mechanical testing, shows that the transparent samples (before) turn white in the gauge region upon deformation (after) (Fig. 3b). This stress whitening observation is consistent with the SEM data and with the formation of micron-sized cavities in PLLA matrix.[30,31]

Rubber toughened thermoplastics often incur a post yield stress drop (PYSD), as a result of necking behaviour after yielding.[44,45] This parameter is important in industrial manufacture and commercialisation. The PYSD is typically at least 10–20 MPa resulting in significant compromises to practical tensile toughness and strength, which are undesirable from application perspective, irrespective of any improvements to elongation at break, or of any increases in stress at break at higher strains in post-yield.[44,45] Here, semi-crystalline PLLA was chosen to reduce these factors.[45] As was demonstrated, adding 7.5 wt% or higher copolymer additive led to PYSD values <5 MPa, and, for the lead material $[\mathbf{P2}_{25}\text{-}\mathbf{PLLA}_{23}]_{15}$, the PYSD was 3 MPa (Fig. 3a).

### Other block polymer compositions in PLLA blends

By exploiting the controlled polymerization catalysis, two further systematic series of block polymers, $[\mathbf{P2}_{x}\text{-}\mathbf{PLLA}_{y}]_{15}$ (Table 1, entries 6–12), were prepared and used to make PLLA blends (Table 2, entries 9 and 12–17). Each of the series were designed to be compared against the lead sample from the first series, *i.e.* $[\mathbf{P2}_{25}\text{-}\mathbf{PLLA}_{23}]_{15}$. In both series, the samples were blended with PLLA at 15 wt% (the optimum additive amount from the first series) and thermal and tensile mechanical characterization conducted. In the second blend series, the block polymer samples feature either variable **PLLA** DP, from 25–125, with fixed **P2** DP of 25, or variable **P2** DP, from 8–25, with fixed **PLLA** DP of 25 (*i.e.* changing $x$ or $y$, Table 1, entries 6–12; Table 2, entries 9, 12–15). The second series was designed to understand the optimum relative chain lengths for the poly(ester-*alt*-ether) or PLLA blocks in the additives. Either increasing the PLLA DP, or decreasing the **P2** DP, led to blends which showed less effective toughening compared with the lead sample, $[\mathbf{P2}_{25}\text{-}\mathbf{PLLA}_{23}]_{15}$ (Table 2, entry 9 *vs.* 12–15). Indeed, plots of the tensile toughness *vs.* the block polymer DP values help to illustrate these trends (Fig. 4). The PLLA blend toughness increases as the DP of the poly(ester-*alt*-ether) increases, reaching a maximum at **P2** DP = 25, and, it decreases as the PLLA block DP increases, having its maximum also at **PLLA** DP = 23 (Fig. 4a). These trends highlight the importance of appropriate block polymer design and are rationalised by the ability to access the optimum block polymer phase-separated micro-structures in the PLLA matrix, in order to deliver the greatest toughening. This rationale is consistent with the SEM data on the different sample fracture surfaces (Fig. S87†).

In the third series, the two blocks have the same relative (molar) composition (1 : 1 or $w_{\mathrm{PLLA}}$ = 0.3) but variable DP values (for both blocks) from 8–25 (variable $x$ + $y$, Table 1, entries 6, 11, 12; Table 2, entries 9, 16, 17). In the case of the two block polymers with lower DP values (lower overall molecular weight), the resulting blends showed inferior tensile mechanical properties compared to $[\mathbf{P2}_{25}\text{-}\mathbf{PLLA}_{23}]_{15}$ (Table 2, entries 9, 16, 17 and Fig. 4b). This finding is tentatively attributed to lower molecular weight samples showing partial miscibility, including between the elastomer block (**P2**) and the PLLA matrix. This notion is supported by the thermal analyses which show lower glass transition temperatures for the blends *vs.* neat PLLA (Table 2, entries 1 *vs.* 16, 17). Overall, plots of tensile toughness *vs.* block polymer DP showed a maximum for the best sample from series 1, *i.e.* $[\mathbf{P2}_{25}\text{-}\mathbf{PLLA}_{23}]_{15}$.

### PLLA blend dynamic mechanical analyses and melt rheology

Dynamic-Mechanical Thermal Analyses (DMTA) were undertaken to monitor the evolution of the PLLA blend storage modulus ($E'$), loss modulus ($E''$) and the damping factor (tan $\delta$) with temperature (Fig. S83 and Table S4†). In these experiments the most effective blend, $[\mathbf{P2}_{25}\text{-}\mathbf{PLLA}_{23}]_{15}$, was compared against the neat PLLA sample, under equivalent conditions (Table 2, entry 1 *vs.* 9). The toughened PLLA blend ($[\mathbf{P2}_{25}\text{-}\mathbf{PLLA}_{23}]_{15}$) shows a plateau in its storage modulus ($E'$), from 30–55 °C, at a value which is only slightly higher for neat PLLA (2.9 *vs.* 2.8 GPa, Fig. 5). Both samples show similar trends in the loss modulus, $E'$, behaviour from 30–120 °C. Over these temperatures the samples are firstly in the glassy region, pass through the glass transition and transform into the rubbery

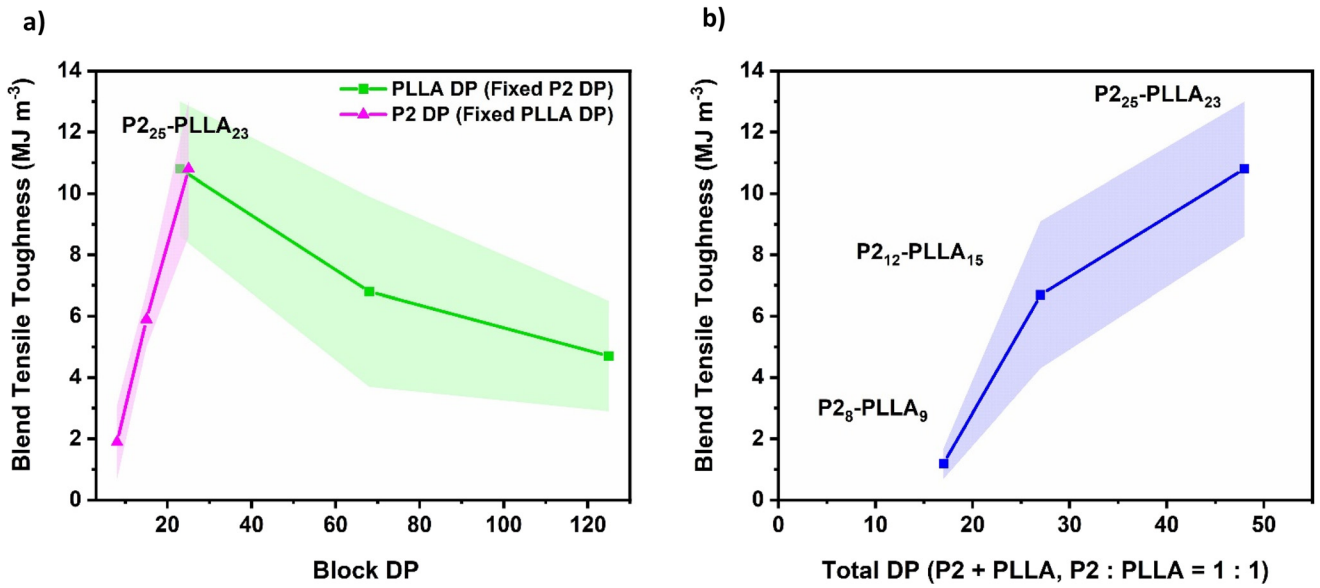


**Fig. 4** Plots to illustrate the influences of block polymer composition (a) and block polymer DP (b) on PLLA toughening (see Table 2 for numerical data and errors, and Fig. S85† for stress *vs.* strain data). Blends of the composition $[P2_x\text{-}PLLA_y]_{15}$ were compared, at a fixed 15 wt% copolymer loading. (a) Plot showing tensile toughening *vs.* block polymer composition for two series of polymers, the first making changes to DP **PLLA** (green squares), while fixing DP **P2**, and the second changing DP **P2** (pink triangles), while fixing DP PLLA. (b) A plot showing PLLA toughening *vs.* overall DP of the block polymer (DP of **P2** (*x*) + DP of PLLA (*y*)), where $x : y = 1 : 1$, while $x + y$ was increased (each data point is the average of 5 tensile measurements). The error range is shown by the shaded regions.

plateau. The similarity of the data suggests there is broadly equivalent mechanical stability between the toughened PLLA blend and pure PLLA (Fig. 5a). Considering the trends in tan $\delta$, the relative magnitude of the damping factor was larger for $[P2_{25}\text{-}PLLA_{23}]_{15}$ compared with PLLA. Comparing the data for the lead blend sample against other compositions show it has the largest magnitude of damping (Fig. 5b and S83†). It has been suggested that the relative magnitude of the tan $\delta$ peak correlates with the materials' ability to dissipate energy.[46,47] Thus, the DMTA findings further substantiate the experimental evidence that the blend $[P2_{25}\text{-}PLLA_{23}]_{15}$ shows the optimum balance between tensile strength (48.7 MPa) and elongation (24.5%).

Rheology frequency sweeps were performed using neat PLLA and $[P2_{25}\text{-}PLLA_{23}]_{15}$ at 170 °C, *i.e.* above the PLLA melting temperature (Fig. 5c and d). The rheological tan $\delta$ decreases linearly with frequency for neat PLLA, suggesting it flows as a viscous liquid (Fig. 5c). On the other hand, $[P2_{25}\text{-}PLLA_{23}]_{15}$ blend behaves similarly to PLLA at higher frequencies (*i.e.* it increases steadily with decreasing frequency) but, unlike neat PLLA, it reaches a plateau in tan $\delta$ at low frequencies (Fig. 5c). The plateau behaviour arises due to an increase in the elastic component of the shear modulus ($G'$), compared to neat PLLA, and is tentatively attributed to block polymer–PLLA interfacial interactions.[46]

Neat PLLA shows complex viscosity ($\eta^*$) *vs.* frequency behaviour which is indicative of a non-Newtonian fluid; it reaches a plateau at lower frequencies (10 300 Pa $s^{-1}$ at $10^{-2}$ Hz) and decreases at higher frequency, indicative of shear thinning behaviour (Fig. 5d).[48] $[P2_{25}\text{-}PLLA_{23}]_{15}$ behaves similarly but shows lower values for the complex viscosity and achieves its plateau at lower on-set frequency (3789 Pa $s^{-1}$ at $10^{-2}$ Hz); *i.e.* it shows a lower frequency onset of shear-thinning (Fig. 5d). The blend sample shows both lower melt viscosity and early onset shear thinning *vs.* neat PLLA, these properties may help reduce process energy input, but must be optimised for specific processing and application methods.

### PLLA blend end-of-life options

As well as being bio-sourced, the (bio)degradability of PLLA is a major benefit.[1] There is also growing interest in recycling PLLA, particularly chemically recycling it to its monomer, L-LA, for applications where wastes are retrievable.[3,32] Given the promising behaviour of the block polymers in toughening commercial PLLA, it's important to establish their influences, if any, over both PLLA chemical recycling to monomer and to its (bio)degradation. Prior development of PLLA toughening agents did not often address experiments to test end-of-life recycling or biodegradation experiments, hence this aspect warrants greater research attention (Fig. 6).[21,25,49]

Chemical recycling of PLLA to L-LA could be important in a future circular plastic economy, helping to reduce greenhouse gas emissions, preserving the L-LA embedded energy and retaining more material value than complete biodegradation.[50] Recently, our team have reported upon a new type of catalysed PLLA recycling, conducted in the polymer melt (130–180 °C), with nitrogen flows used to drive monomer evolution and using low loadings of $Sn(Oct)_2$ as the catalyst (1 : 1000 molar

 

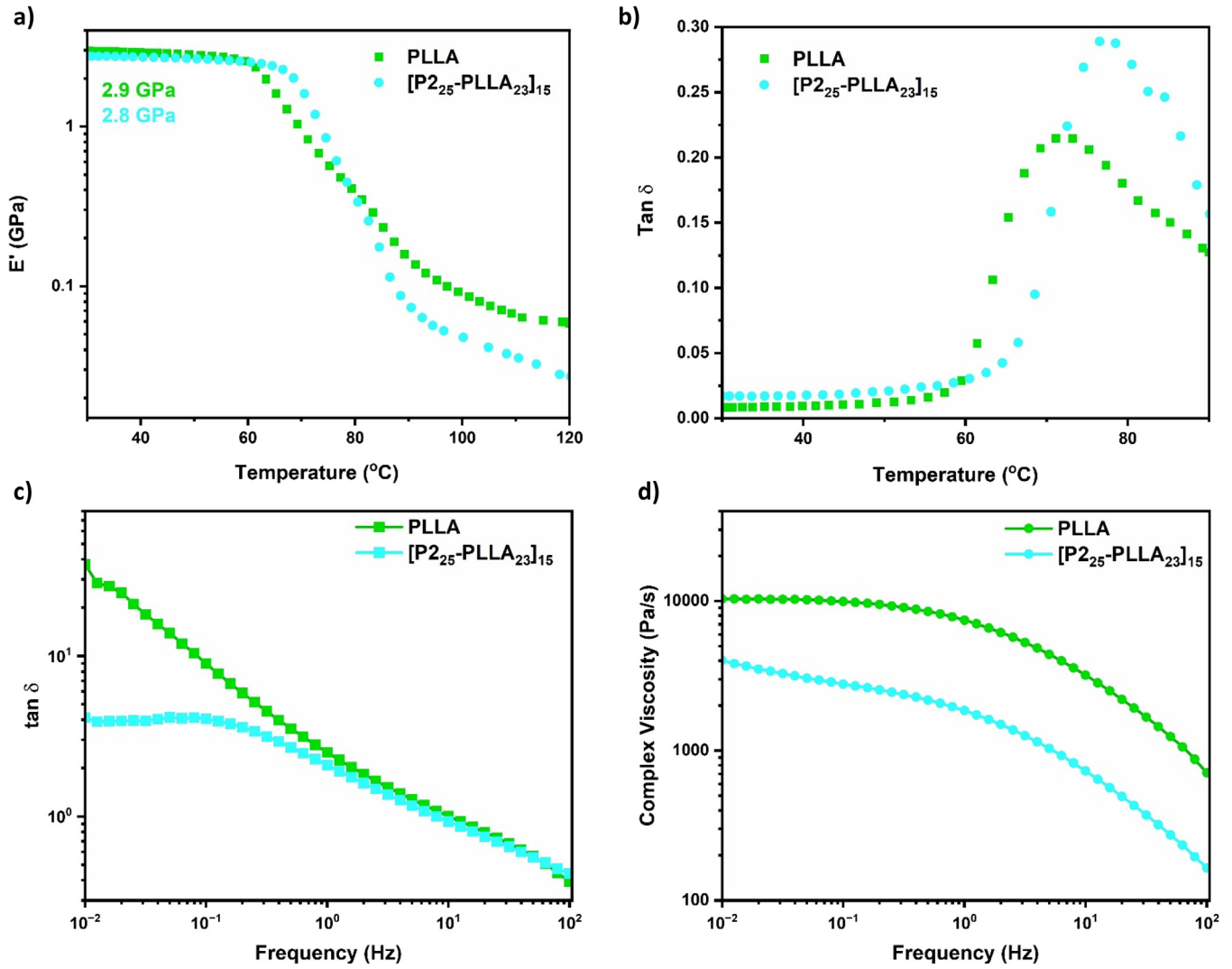


**Fig. 5** Illustrates characterization data for lead sample **[P2$_{25}$-PLLA$_{23}$]$_{15}$** by dynamic thermal mechanical analyses and rheology. (a and b) Plots contrast Storage and tan $\delta$ (damping factors), measured by DMTA, *vs.* temperature for PLLA (green) and **[P2$_{25}$-PLLA$_{23}$]$_{15}$** (blue). Samples were heated from 30–170 °C, at a rate of 2 °C min$^{-1}$, with a frequency of 1 Hz, 0.001 N pre-load force and 0.015% strain amplitude. (c and d) Plots show rheological tan $\delta$ and complex viscosity, ($\eta$*) *vs.* frequency for PLLA (green) and **[P2$_{25}$-PLLA$_{23}$]$_{15}$** (blue). Samples were analysed by melt rheology (170 °C), conducted in the linear viscoelastic region: 1% amplitude strain, 100–0.01 Hz.

loading). Under these conditions, only the monomer L-LA was formed in very high yield, activity and purity (>99% L-LA).[19] The recycling was proposed to occur by a Sn(II) alkoxide catalysed depolymerization process occurring from the PLLA chain-end. Given the success of this methodology using commercial PLLA samples, it was important to establish whether it would also apply to a representative PLLA blend, **[P2$_{25}$-PLLA$_{23}$]$_{10}$** (section S1.2.10–11 and S7†). First, the Sn(Oct)$_2$ catalyst was dispersed into the polymer blend (1 : 1000, solution casting films followed by solvent removal in vacuum oven). The film was heated, in a TGA-IR instrument, at 180 °C with nitrogen flow (25 mL min$^{-1}$). The sample mass loss *vs.* time data was collected and the effluent evaluated using IR spectroscopy (Fig. S94†). Over 150 min, the blend showed 90% mass loss and IR spectroscopy confirmed the sole product was L-LA (Fig. 6b and S94†). The sample did not undergo any further mass loss and the residual mass content (10%) is consistent with the block polymer loading in the original blend (10 wt%). Next, the blend was subjected to laboratory scale chemical recycling using otherwise identical conditions but with nitrogen flow replaced by dynamic vacuum and a sublimation apparatus to collect L-LA (**[P2$_{25}$-PLLA$_{23}$]$_{10}$** = 128 mg, section S1.2.11†). Once again, at this larger-scale the highly selective and complete chemical recycling of the blend occurred, with L-LA isolated in 87% yield (PLLA = 100 mg, Fig. S95†). The product $^1$H NMR spectrum confirms the formation of 95 : 5 L-LA : *meso*-LA, which exactly matches the composition of the commerical PLLA sample (*i.e.* the commercial material contains ~5% *meso*-linkages, Fig. S96†). Mindful of detection limits using NMR spectroscopy, the L-LA purity, and

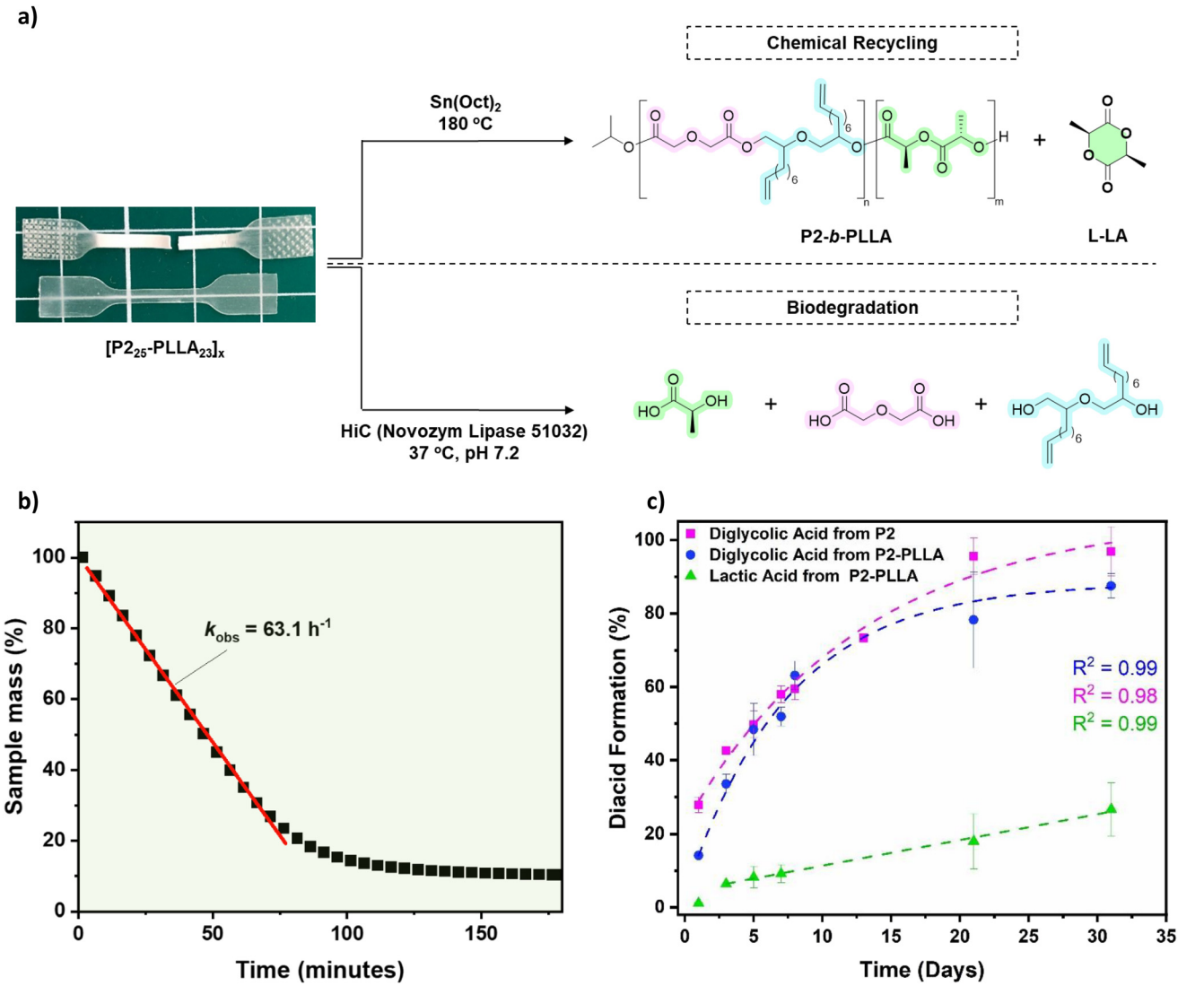


**Fig. 6** Illustrates the chemical recycling and biodegradation routes accessed by the PLLA blends and block polymers. (a) Schematic illustration of the two end-of-life options for toughened PLLA; (i) selective chemical recycling to form **P2$_{25}$-PLLA$_{23}$** and L-LA and (ii) enzymatic degradation (biodegradation) to form L-lactic acid and diglycolic acid (and diol). (b) Plot showing the chemical recycling of **[P2$_{25}$-PLLA$_{23}$]$_{10}$** by sample mass loss data *vs.* time. Recycling conditions: Sn(Oct)$_2$ : polymer, 1 : 1000, 180 °C, $N_2$ flow at 25 mL min$^{-1}$ (L-LA TGA-IR spectrum, Fig. S94†). (c) Plot showing acid formation (DGA or L-LA) *vs.* time for the biodegradation of **P2** and **P2-PLLA**. Biodegradation conditions: *Humicola insolens* Cutinase (HiC), polymer : cutinase = 1 : 2 (by weight), acid formation was measured by HPLC-RI detection calibrated for diglycolic acid (pink squares from **P2** and blue circles from **P2-PLLA**) and L-lactic acid (green triangles from **P2-PLLA**). Samples were incubated at 37 °C and pH 7.2, with a 0.05 M phosphate buffer. Degradation rate data are fit to exponentials (diglycolic acid) and linear fits (L-lactic acid).

stereochemistry, was also assessed suing GC-MS (Fig. S97†). Both monomer characterization data suggest that the blend is efficiently chemically recycled without any L-LA epimerization. Further, in the laboratory scale experiment the bulk PLLA was efficiently recycled and the **P2$_{25}$-PLLA$_{23}$** block copolymer was separated and identified after the reaction, providing a future re-use option. To test this, a polymer blend (**[P2$_{25}$-PLLA$_{23}$]$_{25}$**, 600 mg) was chemically recycled (as above). L-LA was collected in 80% yield (section S7.1†). $^1$H and $^{31}$P{$^1$H} NMR spectroscopy suggested that the recyclate (left in the reaction flask) was a mixture of the block polymer additive and a small quantity of residual PLLA (2 equivalents of poly(L-lactide) per ABB repeat unit, Fig. S98 and 99†). The catalyst was removed *via* a silica plug and the recylate was subsequently re-blended with high molar mass PLLA (following procedures in section S3.0†) with 15 wt% **P2$_{25}$-PLLA$_{23}$** block polymer. The thermal-mechanical properties were checked by DSC and DMTA and compared to neat PLLA and **[P2$_{25}$-PLLA$_{23}$]$_{15}$** pre-recycling values above (Table S9†). After recycling, the **[P2$_{25}$-PLLA$_{23}$]$_{15}$** $T_g$ (60 °C) and crystallinity of (38%) remained high (Table S9†). The tensile storage modulus ($E'$) of the recycled **[P2$_{25}$-PLLA$_{23}$]$_{15}$** blend was measured as 2.6 GPa at −60 °C, before dropping to 2.3 GPa after passing through the $T_g$ of the **P2$_{25}$-PLLA$_{23}$** dispersed phase (−46 °C from tan $\delta$), reaching 2.2 GPa at 25 °C (Fig. S100

 

and 101†). This is slightly lower than discussed above for $[\mathbf{P2_{25}\text{-}PLLA_{23}}]_{15}$ pre-recycling ($E'$ = 2.8 GPa) and for neat PLLA ($E'$ = 2.9 GPa) (Table S9 and Fig. S100 and 101†). This slight drop in modulus may be due to the residual lower molar mass PLLA added (which remained in the recyclate, and was subsequently blended), any residual Sn(II) catalyst, or, to minor contamination by particulate matter (dust), reducing the materials stiffness by causing defects. These effects are harder to control on small scales, and recycling on a larger scale would be expected to eliminate such issues. These experiments demonstrate the potential for future re-use of the diblock polymer additive following selective chemical recycling of PLLA to L-LA.

To test for (bio)degradation, *in vitro* enzyme catalysed hydrolysis reactions were conducted using (separately) samples of **P2** (poly(ester-*alt*-ether)), $\mathbf{P2_{25}\text{-}PLLA_{23}}$ block copolymer, $[\mathbf{P2_{25}\text{-}PLLA_{23}}]_{15}$ blend or semicrystalline **PLLA**. The (bio)degradation experiments all applied an esterase, *Humicola insolens* Cutinase, with samples exposed to the enzyme as a viscous liquid (**P2**), soft solid ($\mathbf{P2_{25}\text{-}PLLA_{23}}$) or as films ($[\mathbf{P2_{25}\text{-}PLLA_{23}}]_{15}$ and PLLA). The samples were all incubated in the aqueous solutions at 37 °C, with pH controlled at 7.2 by use of phosphate buffer (section S1.2.12†). The enzyme was selected due to its precedent in PLLA and aliphatic polyester degradations (HiC, trademark name Novozym 51032).[51,52] Indeed, there is quite a substantial literature detailing PLLA enzymatic degradation, allowing for the commercial sample to serve as an appropriate benchmark when examining degradation chemistry of the new polymers.[15] The extent of the (bio)degradations were monitored by regular aliquot analysis by HPLC, equipped with an RI detector, which was calibrated for both diglycolic acid (from **P2**) and L-lactic acid (Fig. S102–104†).[51,53] In addition to the HPLC calibration, the hydrolysis fractions were collected and analysed by ESI-MS to confirm purity (S1.2.12, Fig. S107 and S110–111†).

The (bio)degradation experiments showed steady increases in the acidic degradation products, allowing for monitoring of polymer conversion *vs.* time data (Fig. 6b). Over 31 days, the poly(ester-*alt*-ether) **P2** achieved 97% degradation and the block polymer **P2-PLLA** resulted in 88% degradation of the **P2** block and 27% degradation of the **PLLA** block (Fig. 6c and Fig. S105–106†). The presence of the ether-diol, also from the degradation of **P2** (Fig. 6a), was confirmed by mass spectrometry (negation ion mode) of the dried degradation reaction (Fig. S110†). Films of $[\mathbf{P2_{25}\text{-}PLLA_{23}}]_{15}$ and of neat **PLLA**, incubated with the enzyme under the same conditions, degraded significantly more slowly, as would be expected due to the high molecular weight PLLA, which is the majority component in both cases (Fig. S108 and S109†). It is well-known that PLLA molecular weight, crystallinity and film surface area all influence the relative biodegradation rates.[54] Given these constraints, we used the (bio)degradation experiments for these samples to provide qualitative evidence supporting additive (block polymer) degradability. Over 34 days, the lead blend sample $[\mathbf{P2_{25}\text{-}PLLA_{23}}]_{15}$ showed ~23% **P2** degradation, demonstrating that blending does not hinder the effective (bio)degradation of the block polymer additive (Fig. S108†). The toxicity of the small molecule ether-diol degradation product is not addressed in this study, and, we make no evaluation of toxicity.

## Discussion

This paper presents a new series of block polymer rubber toughening additives for commercial, high molar mass PLLA. The block polymers were efficiently synthesised, using a single process and catalyst, from commercial monomers. They showed effective PLLA toughening, maintaining its high tensile strength, crystallinity, thermal transitions ($T_g$ and $T_m$) and stiffness, whilst increasing its elongation at break and substantially toughening it. The PLLA blends are all chemically recyclable to L-lactide, with the block polymer being retained after recycling allowing for its re-use. The block polymer additives are also (bio)degradable, forming di-acids and diols, as well as L-lactic acid during enzymatic degradation.

To evaluate and contextualise the performance of these PLLA blends, it's appropriate to compare them against the leading toughend PLLA samples, reported in the literature. As outlined in the introduction, there are a range of PLLA toughening approaches but rubber/elastomer toughening is particularly promising when it delivers stable blends.[21,25] When making comparisons, it's important to note that some prior toughening studies applied amorphous (racemic) PLA. In these cases, direct comparisons with PLLA are not possible, since the semi-crystalline polymer tends to show much lower elongation at break values.[31] Nonetheless, it is very important to establish toughening strategies for PLLA since its commercial applications rely on its greater tensile modulus/strength (than PLA). Furthermore, when considering/evaluating PLLA as a potential substitute for current plastics, *e.g.* polystyrene (see below), achieving a high melting temperature is important. An excellent prior investigation into PLLA rubber toughening, by Bates and co-workers, applied semi-crystalline, high molecular weight PLLA, with just 5 wt% of a polyether elastomer, PEO-PBO (PEO = polyethylene oxide; PBO = polybutylene oxide).[20] The blends show impressive tensile strength and modulus (49 MPa and 2.9 GPa, respectively) and elongation at break at 14%.[5] In our work, the **P2-PLLA** block polymer is added at higher (15 wt% or 11 wt% **P2**) loading into high molecular weight, semi-crystalline PLLA. High strength and modulus was achieved at 48.7 MPa and 3.1 GPa, respectively, and the elongation at break values reached 25%. In addition, it is useful that the block polymer structure delivers equivalent PLLA crystallinity (42%), glass transition ($T_g$ = 63 °C), and melt temperatures ($T_m$ = 149 °C) to neat PLLA. Our results are similar to the inspiring work from Bates and co-workers and, as an added benefit, our block polymers are also (bio) degradable.

To compare PLLA against various different grades of PS, ABS and HIPS, we collated commercial data-sheets and used them to construct an Ashby plot (Fig. 7a and section S9†). For

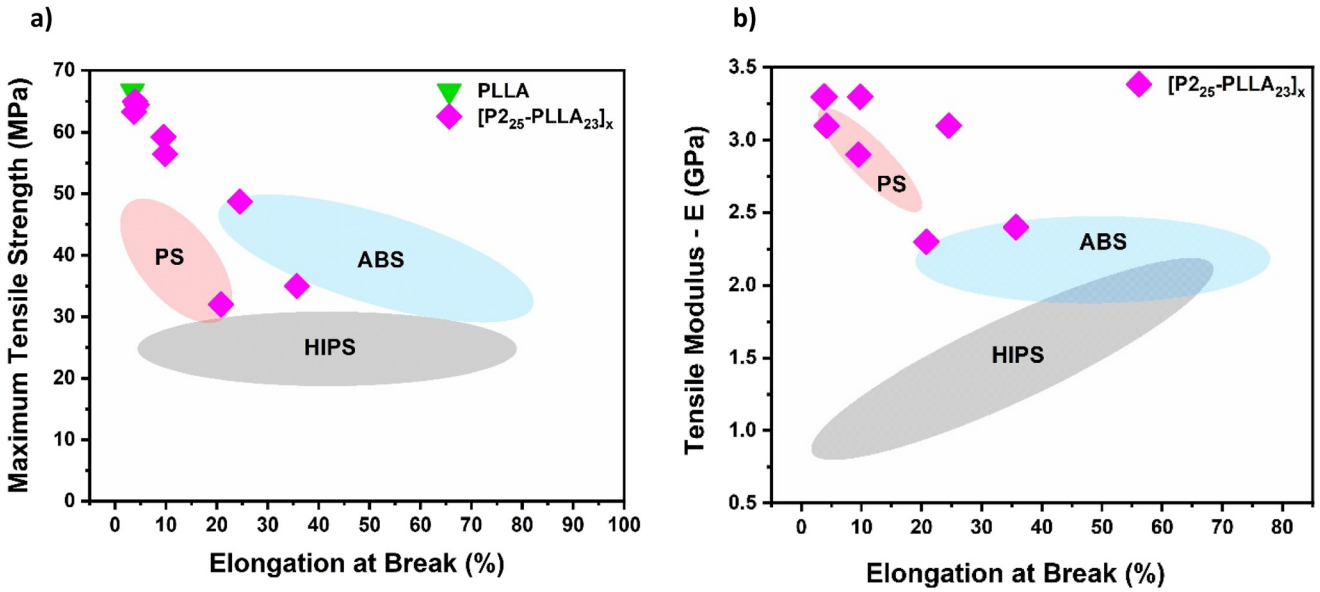


**Fig. 7** Presents plots contextualising PLLA samples in this work with commercial thermoplastics, particularly polystyrene classes. (a) Ashby Plot showing tensile mechanical property regions (tensile strength (MPa) *vs.* elongation at break (%)) and (b) tensile modulus (GPa) *vs.* elongation at break (%), for polystyrene, PS (red), poly(acrylonitrile-butadiene-styrene), ABS (blue), high-impact polystyrene, HIPS (grey) and **PLLA** samples in this work (pink diamonds for blends *vs.* green triangle for pure PLLA).

example, analyses of these different data-sheets shows that commercial PS samples show tensile strengths from 23–47 MPa but low elongation at breaks from 3–21%. Using the Ashby plots allows for benchmarking and comparison of the toughened PLLA tensile mechanical properties against those of currently used commercial polystyrenes (Fig. 7a). Depending on the quantity of the block polymer additive, the PLLA blends show tensile strengths and elongations at break which fall into the properties exhibited by either pure PS, or toughened samples like ABS/HIPS (Fig. 7a). In these blends, adding 1–10 wt% of the block polymers delivers PLLA samples which are more closely aligned to high strength PS. Whilst, adding more block polymer (15–25 wt%) forms PLLA samples which align with some grades of ABS; the sample with 20 wt% is close to the properties of both ABS and HIPS (Fig. 7a). The tensile modulus ($E$) and elongation ($\varepsilon_B$) also closely align with PS, for PLLA blends with between 1–10 wt% block polymer additive (Fig. 7b). For blends with 15, 20 and 25 wt% additive, the elongation increases to lower-to-middle ABS and HIPS values, while the modulus remains higher, more comparable to PS or ABS (Fig. 7b). The lead sample **[P2$_{25}$-PLLA$_{23}$]$_{15}$** (15 wt% polymer additive) for instance, showed a modulus on par with PS (3.1 GPa), although an elongation that is more akin to HIPS (24.5%), that is, the material is as strong as PS, although as ductile as some grades of HIPS (Fig. 7b). This is achieved with 11 wt% of poly(ester-*alt*-ether) additive (as the rest of the block polymer is PLLA), which is in-line with 3–10 wt% of PB commonly used in HIPS.[55]

Whilst Ashby plots are very helpful in providing visual maps of property space, they inevitably risk some over-looking of other critical properties. To allow for a broader evaluation of the toughened PLLA samples, a line graph compares the high temperature service limit for these thermoplastics (Fig. 8). The diagram helps to illustrate that for some applications, PLLA temperature stability may be an issue, *e.g.* PLLA $T_g$ (63 °C) is lower than for PS ($T_g$ = 94 °C), ABS ($T_g$ = 110 °C) and HIPS ($T_g$ = 100 °C, see Fig. 8). On the other-hand, the high temperature melt of PLLA, and the **[P2$_{25}$-PLLA$_{23}$]$_x$** PLLA blends may be helpful in some circumstances.

One important potential future benefit to these toughened PLLA samples is their ability to undergo chemical or biological

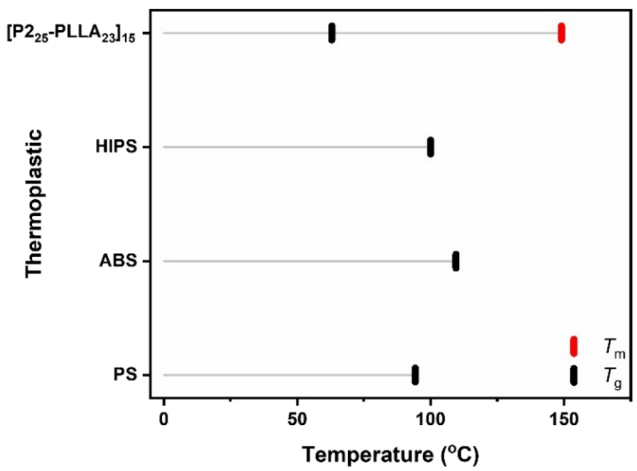


**Fig. 8** Line graph showing upper temperature limits (service) for commercial polystyrene samples and lead PLLA samples from this work.

depolymerizations (biodegradation). Here, we demonstrated that **P2**, **$P2_{25}$-$PLLA_{23}$**, and blends with PLLA were all enzymatically degradable using a cutinase enzyme, at 37 °C. Also, the blends were efficiently chemically recycled to L-lactide (100% selective), at 180 °C and in ~2 hours, with retention of the block polymer for future re-use in blends. Naturally, such (bio) degradation is not feasible using PS, ABS or HIPS, nor are there equivalent low temperature, high selectivity chemical recycling approaches using these commercial plastics (and any recycling is challenging for ABS and HIPS).[5,9,10,56] Chemical recycling of PS is feasible at 310–350 °C, with 33–80% polystyrene consumption.[9,13,56] Nonetheless styrene selectivity can be very challenging, with other mono- and poly-aromatic side-products commonly reported.[9] The chemical recycling of ABS and HIPS is even more complex, with PB particles damaged (charred) during the reaction and maximum styrene yields well under 50%.[7] Industrially, PS pyrolysis is feasible at 800 °C.[7,9] Alternative reports of lower energy processes, *e.g.* photo-excitation/oxidation, produce oxidised aromatic products in 23–71% yields.[57–59] Mechanical recycling for these PS-based copolymers and blends is also extremely complicated, or not feasible, and end-life biodegradation is not possible. Therefore, applications where material end-life recycling and/or (bio)degradation are desirable may benefit from the approaches in this work and by testing toughened PLLA samples.

The block polymers, used to toughen the PLLA, were all synthesised in a one-pot switch catalysis process. This is important since it obviates additional synthetic and purification steps and may simplify larger-scale materials production. This manuscript establishes a general, and new, protocol to make poly(ester-*alt*-ether)-*b*-PLLA samples. Both the poly(ester-*alt*-ether) ROCOP and L-LA ROP are controlled polymerizations, prepared using the same catalyst; these atom efficient and selective processes facilitate structure–property investigations. The process occurs at moderate/low temperature (50 °C) without any organic solvent, the excess epoxide helps maximise rates and could be recycled at larger-scale. In terms of future monomer sourcing: L-LA is already sourced from starch biomass; PLLA is already produced from starch rich biomass; diglycolic anhydride (DGA), maleic anhydride (MA) and 1,2-epoxy-9-decene (ED) are all commercial products and all have routes demonstrated from renewable starting materials.[38]

In future, other related block polymers to those described here should be tested to produce new materials and try to map the property (and application) space for current plastics. The synthetic route to these block polymers should be amenable to other commercial and bio-based monomers, like epoxides, anhydride and/or cyclic esters.[39] Another important priority is to deliver fully bio-based additives, in this regard there is already literature outlining routes to both DGA and ED from biomass sources which could be a useful starting point for future optimizations.[39,60] The block polymer rubber toughening strategy should also be used, in future, to improve ductility for other bio-based (*e.g.* PHB) and, even, $CO_2$-derived plastics.

# Conclusions

A series of new block polymers, poly(ester-*alt*-ethers)-*b*-PLLA, are highly effective in toughening high molecular weight, semi-crystalline, commercial poly(L-lactide) PLLA. The block polymers were synthesised, using a solvent free, low temperature, catalysed one-pot process, from commercial anhydrides, epoxides and L-lactide; all monomers were chosen on the basis of being, or having strong future potential to be, renewably sourced. This first report of poly(ester-*alt*-ether)-*b*-PLLA synthesis demonstrates the control, versatility and high selectivity of the catalysis. Using these controlled polymerizations yielded a systematic series of well-defined block polymers, featuring variable block compositions, degrees of polymerization and chemistries. These block polymers were blended with commercial PLLA and the toughened samples were evaluated using a comprehensive series of thermal, tensile mechanical and rheological methods. The lead sample featured 15 wt% block polymer (11 wt% poly(ester-*alt*-ether) in PLLA); it combines both high tensile modulus ($E$ = 3.1 ± 0.1 GPa) and tensile strength (48.7 ± 1.2 MPa) with significantly greater ductility (7× higher) and tensile toughness (8× higher) than commercial PLLA alone. The toughened PLLA blend retained equivalent thermal properties ($T_g$, $T_m$), crystallinity and thermal stability to PLLA. The toughened PLLA blends were efficiently chemically recycled, using a catalytic process in the polymer melt, to produce the monomer, L-lactide in very high conversion and selectivity. The new chemical recycling process also separates the block polymer, providing a future pathway for its re-use. The lead block polymer underwent complete enzymatically catalysed hydrolysis over 30 days to form diglycolic acid, diol and L-lactic acid. These toughened PLLA samples have thermal-mechanical properties which are in the range of polystyrene, poly(acrylonitrile-butadiene-styrene) or even high-impact polystyrene. Many of these polystyrene-based materials lack closed-loop recycling options and are not biodegradable. The toughened PLLA materials may, therefore, serve as suitable substitutes for currently used PS-based plastics and are particularly recommended where end-life recycling and/or biodegradation are important. In future, the synthesis–property–recycling–degradation methods and approach described in this work are expected to be much more broadly applicable, both to a range of other block polymer compositions and to the toughening of other bio-based and $CO_2$-derived plastics.

# Conflicts of interest

There are no conflicts to declare.

# Data availability

The data supporting this article have been included as part of the ESI or are available upon request.†

## Acknowledgements

The EPSRC (EP/S018603/1, EP/R027129/, EP/Z532782/1, EP/V038117/1), Research England (Innovation Centre for Advanced Sustainable Technologies, iCAST), Innovate UK (Project: Economiser), the Oxford Martin School (Future of Plastics) and the James Fairfax Oxford-Australia Scholarship are acknowledged for research funding.

## References

1 F. Vidal, E. R. van der Marel, R. W. F. Kerr, C. McElroy, N. Schroeder, C. Mitchell, G. Rosetto, T. T. D. Chen, R. M. Bailey, C. Hepburn, C. Redgwell and C. K. Williams, *Nature*, 2024, **626**, 45–57.
2 D. K. Schneiderman and M. A. Hillmyer, *Macromolecules*, 2017, **50**, 3733–3749.
3 Y. Zhu, C. Romain and C. K. Williams, *Nature*, 2016, **540**, 354–362.
4 J.-G. Rosenboom, R. Langer and G. Traverso, *Nat. Rev. Mater.*, 2022, **7**, 117–137.
5 Z. O. G. Schyns and M. P. Shaver, *Macromol. Rapid Commun.*, 2021, **42**, 2000415.
6 S. R. Nicholson, N. A. Rorrer, A. C. Carpenter and G. T. Beckham, *Joule*, 2021, **5**, 673–686.
7 N. S. Giakoumakis, C. Vos, K. Janssens, J. Vekeman, M. Denayer, F. D. Proft, C. Marquez and D. D. Vos, *Green Chem.*, 2024, **26**, 340–352.
8 M. Mathew and S. Thomas, *Polymer*, 2003, **44**, 1295–1307.
9 M. T. Chin and T. Diao, *ACS Catal.*, 2024, **14**, 12437–12453.
10 A. Rahimi and J. M. García, *Nat. Rev. Chem.*, 2017, **1**, 1–11.
11 M. Fischer and G. P. Hellmann, *Macromolecules*, 1996, **29**, 2498–2509.
12 E. R. Wagner and L. M. Robeson, *Rubber Chem. Technol.*, 1970, **43**, 1129–1137.
13 A. Schade, M. Melzer, S. Zimmermann, T. Schwarz, K. Stoewe and H. Kuhn, *ACS Sustainable Chem. Eng.*, 2024, **12**, 12270–12288.
14 J. Hopewell, R. Dvorak and E. Kosior, *Philos. Trans. R. Soc., B*, 2009, **364**, 2115–2126.
15 X. Zhang, M. Fevre, G. O. Jones and R. M. Waymouth, *Chem. Rev.*, 2018, **118**, 839–885.
16 R. M. Cywar, N. A. Rorrer, C. B. Hoyt, G. T. Beckham and E. Y.-X. Chen, *Nat. Rev. Mater.*, 2022, **7**, 83–103.
17 European Bioplastics, **https://www.european-bioplastics.org/bioplastics/materials/**, accessed 22 January 2025.
18 M. Dusselier, P. V. Wouwe, A. Dewaele, E. Makshina and B. F. Sels, *Energy Environ. Sci.*, 2013, **6**, 1415–1442.
19 T. M. McGuire, A. Buchard and C. Williams, *J. Am. Chem. Soc.*, 2023, **36**, 19840–19848.
20 C. J. McCutcheon, B. Zhao, C. J. Ellison and F. S. Bates, *Macromolecules*, 2021, **54**, 11154–11169.
21 K. S. Anderson, K. M. Schreck and M. A. Hillmyer, *Polym. Rev.*, 2008, **48**, 85–108.
22 M. Razavi and S.-Q. Wang, *Macromolecules*, 2019, **52**, 5429–5441.
23 R. Auras, B. Harte and S. Selke, *Macromol. Biosci.*, 2004, **4**, 835–864.
24 C. O. Tuck, E. Pérez, I. T. Horváth, R. A. Sheldon and M. Poliakoff, *Science*, 2012, **337**, 695–699.
25 X. Zhao, H. Hu, X. Wang, X. Yu, W. Zhou and S. Peng, *RSC Adv.*, 2020, **10**, 13316–13368.
26 V. Nagarajan, A. K. Mohanty and M. Misra, *ACS Sustainable Chem. Eng.*, 2016, **4**, 2899–2916.
27 A. Höglund, M. Hakkarainen and A.-C. Albertsson, *Biomacromolecules*, 2010, **11**, 277–283.
28 L. Zimmermann, G. Dierkes, T. A. Ternes, C. Völker and M. Wagner, *Environ. Sci. Technol.*, 2019, **53**, 11467–11477.
29 M. Nofar, Chapter 7 - PLA binary blends with elastomeric polymers, in *Multiphase Polylactide Blends*, Elsevier, 2021, pp. 265–287.
30 B. P. Panda, S. Mohanty and S. K. Nayak, *Polym.-Plast. Technol. Eng.*, 2015, **54**, 462–473.
31 T. Li, J. Zhang, D. K. Schneiderman, L. F. Francis and F. S. Bates, *ACS Macro Lett.*, 2016, **5**, 359–364.
32 C. J. McCutcheon, B. Zhao, K. Jin, F. S. Bates and C. J. Ellison, *Macromolecules*, 2020, **53**, 10163–10178.
33 M. C. Larson, J. P. Coote, F. S. Bates and C. J. Ellison, *Macromolecules*, 2024, **19**, 9334–9345.
34 B. Zhao, C. J. McCutcheon, K. Jin, I. Lyadov, A. J. Zervoudakis, F. S. Bates and C. J. Ellison, *ACS Appl. Polym. Mater.*, 2022, **4**, 8705–8714.
35 L. Gu, E. E. Nessim, T. Li and C. W. Macosko, *Polymer*, 2018, **156**, 261–269.
36 D. W. Grijpma, R. D. A. Van Hofslot, H. Supèr, A. J. Nijenhuis and A. J. Pennings, *Polym. Eng. Sci.*, 1994, **34**, 1674–1684.
37 J. P. Coote, M. C. Larson, F. S. Bates and C. J. Ellison, *ACS Macro Lett.*, 2025, **14**, 80–86.
38 R. W. F. Kerr and C. K. Williams, *J. Am. Chem. Soc.*, 2022, **144**, 6882–6893.
39 R. W. F. Kerr, A. R. Craze and C. K. Williams, *Chem. Sci.*, 2024, **15**, 11617–11625.
40 A. C. Deacy, G. L. Gregory, G. S. Sulley, T. T. D. Chen and C. K. Williams, *J. Am. Chem. Soc.*, 2021, **143**, 10021–10040.
41 T. Stößer, G. S. Sulley, G. L. Gregory and C. K. Williams, *Nat. Commun.*, 2019, **10**, 2668.
42 C. Romain, Y. Zhu, P. Dingwall, S. Paul, H. S. Rzepa, A. Buchard and C. K. Williams, *J. Am. Chem. Soc.*, 2016, **138**, 4120–4131.
43 T. Stößer, D. Mulryan and C. K. Williams, *Angew. Chem., Int. Ed.*, 2018, **57**, 16893–16897.
44 I. N. Haugan, B. Lee, M. J. Maher, A. Zografos, H. J. Schibur, S. D. Jones, M. A. Hillmyer and F. S. Bates, *Macromolecules*, 2019, **52**, 8878–8894.
45 H. Ye, A. Li, G. Li, K. Li, J. Zhang, D. Wang, S. S. Ray, H. Wang and Y. Li, *Macromolecules*, 2024, **57**, 9999–10015.
46 H. Gramespacher and J. Meissner, *J. Rheol.*, 1992, **36**, 1127–1141.

 

47 L.-I. Palade, H. J. Lehermeier and J. R. Dorgan, *Macromolecules*, 2001, **34**, 1384–1390.
48 R. Yang, C. Cai, X. Han, Z. Chen, G. Gu, C. Zhang, G. Zou and J. Li, *Macromolecules*, 2023, **56**, 7271–7285.
49 M. Wang, Y. Wu, Y.-D. Li and J.-B. Zeng, *Polym. Rev.*, 2017, **57**, 557–593.
50 G. W. Coates and Y. D. Y. L. Getzler, *Nat. Rev. Mater.*, 2020, **5**, 501–516.
51 M. Eck, S. T. Schwab, T. F. Nelson, K. Wurst, S. Iberl, D. Schleheck, C. Link, G. Battagliarin and S. Mecking, *Angew. Chem., Int. Ed.*, 2023, **62**, e202213438.
52 Q. Huang, S. Kimura and T. Iwata, *Biomacromolecules*, 2023, **24**, 5836–5846.
53 K. Haernvall, S. Zitzenbacher, H. Amer, M. T. Zumstein, M. Sander, K. McNeill, M. Yamamoto, M. B. Schick, D. Ribitsch and G. M. Guebitz, *Biotechnol. J.*, 2017, **12**, 1600741.
54 T. Iwata, H. Abe and Y. Kikkawa, in *Poly(Lactic Acid)*, John Wiley & Sons, 2010, pp. 383–399.
55 N. S. Giakoumakis, C. Vos, K. Janssens, J. Vekeman, M. Denayer, F. D. Proft, C. Marquez and D. D. Vos, *Green Chem.*, 2024, **26**, 340–352.
56 Z. Chen, Y. Kimura and D. T. Allen, *ACS Sustainable Resour. Manage.*, 2024, **1**, 930–938.
57 S. Xu, S. Liu, W. Song and N. Zheng, *Green Chem.*, 2024, **26**, 1363–1369.
58 Z. Huang, M. Shanmugam, Z. Liu, A. Brookfield, E. L. Bennett, R. Guan, D. E. Vega Herrera, J. A. Lopez-Sanchez, A. G. Slater, E. J. L. McInnes, X. Qi and J. Xiao, *J. Am. Chem. Soc.*, 2022, **144**, 6532–6542.
59 S. Oh and E. E. Stache, *J. Am. Chem. Soc.*, 2022, **144**, 5745–5749.
60 S. Paul, Y. Zhu, C. Romain, R. Brooks, P. K. Saini and C. K. Williams, *Chem. Commun.*, 2015, **51**, 6459–6479.